

University of Windsor

Scholarship at UWindor

Electronic Theses and Dissertations

Theses, Dissertations, and Major Papers

2019

Characterizing phenotypic effects of Spy1 mediated lateral branching

Iulian Eric Derecichei
University of Windsor

Follow this and additional works at: <https://scholar.uwindsor.ca/etd>

Recommended Citation

Derecichei, Iulian Eric, "Characterizing phenotypic effects of Spy1 mediated lateral branching" (2019).
Electronic Theses and Dissertations. 7693.
<https://scholar.uwindsor.ca/etd/7693>

This online database contains the full-text of PhD dissertations and Masters' theses of University of Windsor students from 1954 forward. These documents are made available for personal study and research purposes only, in accordance with the Canadian Copyright Act and the Creative Commons license—CC BY-NC-ND (Attribution, Non-Commercial, No Derivative Works). Under this license, works must always be attributed to the copyright holder (original author), cannot be used for any commercial purposes, and may not be altered. Any other use would require the permission of the copyright holder. Students may inquire about withdrawing their dissertation and/or thesis from this database. For additional inquiries, please contact the repository administrator via email (scholarship@uwindsor.ca) or by telephone at 519-253-3000ext. 3208.

Characterizing phenotypic effects of Spy1 mediated lateral branching

By

Iulian Eric Derecichei

A Thesis

Submitted to the Faculty of Graduate Studies
through the Department of Biological Sciences
in Partial Fulfillment of the Requirements for
the Degree of Master of Science
at the University of Windsor

Windsor, Ontario, Canada

2019

© 2019 Iulian Eric Derecichei

Characterizing phenotypic effects of Spy1 mediated lateral branching

by

Iulian Eric Derecichei

APPROVED BY:

M. Krause
Faculty of Human Kinetics

M. Crawford
Department of Biological Sciences

L. Porter, Advisor
Department of Biological Sciences

September 20th, 2018

DECLARATION OF CO-AUTHORSHIP

I. Co-Authorship

I hereby declare that this thesis incorporates material that is result of joint research, as follows: *Figure 3. and Figure 6. contains research done jointly with Dr. Bre-Anne Fijfield under the supervision of Dr. Lisa Porter. Dr. Fijfield designed and implemented the experiment. Analysis was done by the author.*

I am aware of the University of Windsor Senate Policy on Authorship and I certify that I have properly acknowledged the contribution of other researchers to my thesis and have obtained written permission from each of the co-author(s) to include the above material(s) in my thesis.

I certify that, with the above qualification, this thesis, and the research to which it refers, is the product of my own work.

II. General

I declare that, to the best of my knowledge, my thesis does not infringe or violate the copyright, proprietary rights or any ideas, techniques, quotations from the work of other people, published or otherwise. The work of others is fully acknowledged in accordance with the standard referencing practices. Furthermore, to the extent that I have included copyrighted material that surpasses the bounds of fair dealing within the meaning of the Canada Copyright Act, I certify that I have obtained a written permission from the copyright owner(s) to include such material(s) in my thesis.

I declare that this is a true copy of my thesis, including any final revisions, as approved by my thesis committee and the Graduate Studies office, and that this thesis has not been submitted for a higher degree to any other University or Institution.

ABSTRACT

Mammary development is a continuous and cyclic process that is under tight regulatory control from hormones and cell cycle regulators to mediate transition from the various proliferative, differential and apoptotic steps. Puberty is a time-point of high proliferation during development that has higher susceptibility to breast cancer. Spy1 is a cyclin-like protein known to regulate mammary development and increase proliferation with previous work also showing Spy1 increases tumor susceptibility and pubertal lateral side branching. In this work we demonstrate that elevated levels of Spy1 in puberty significantly increase the number of lateral branches and total epithelial content in mice. Similarly, the pubertal glands saw increased levels of amphiregulin and proliferation. Furthermore, it was demonstrated that elevated Spy1 levels can increase budding in HC11 3D culture and increase total size in primary cell organoids. This data revealed the unique ability of Spy1 to manipulate developmental pathways in the mammary gland.

DEDICATION

This work I dedicate to my family, whose loving support has seen given me strength to succeed in all my endeavours. To my girlfriend Chelsea who has supported me through the long hours of work. To my friends who have given me good advice and been there through my struggles.

ACKNOWLEDGEMENTS

I would like to acknowledge Dr. Lisa Porter for her guidance and help in directing my work. I would not have been able to finish this work without her support and patience. I would also like to thank my committee members Dr. Crawford and Dr. Krause for their continued advice and critique of my work.

I would like to acknowledge Dr. Bre-Anne Fijfield for her teaching, help and guidance throughout this MSc. All the techniques and methodologies I have acquired in this lab I have done thanks to her efforts.

Finally, I would like to acknowledge the Porter lab group. Every single person has been supportive and kind to me as I learned and grew into the person I am today.

TABLE OF CONTENTS

DECLARATION OF CO-AUTHORSHIP / PREVIOUS PUBLICATION.....	iii
ABSTRACT.....	iv
DEDICATION	v
ACKNOWLEDGEMENTS.....	vi
LIST OF TABLES.....	x
LIST OF FIGURES.....	xi
LIST OF APPENDICES	xii
LIST OF ABBREVIATIONS/SYMBOLS	xiii
Introduction	1
<i>The Mammary Gland</i>	1
<i>Mouse Mammary Development in Embryogenesis and Puberty</i>	2
<i>Branching Morphogenesis and Lateral Branching</i>	5
<i>Molecular Signaling in Mammary Proliferation</i>	9
<i>Pregnancy and Lactation</i>	9
<i>Involution</i>	10
<i>Mammary Stem Cells in the Adult Gland</i>	11
<i>Tumor Susceptibility and Abnormal Mammary Development</i>	14
<i>The Cell Cycle</i>	15
<i>CDKs, Cyclins and CKIs</i>	16
<i>SPDYA/Spy1</i>	17
<i>Spy1 and Mammary Development</i>	21
<i>Transgenic Mouse Models</i>	22
<i>Mouse Mammary Tumor Virus and Organ Specific Mouse Models</i>	23
<i>Mammary Organoids, 3D culture and In-vitro models</i>	24

Hypothesis & Objectives	25
Materials and Methods.....	26
<i>Mouse Maintenance</i>	26
<i>Immunohistochemistry</i>	26
<i>Immunofluorescence</i>	27
<i>Mammary Line Maintenance</i>	27
<i>Plasmids and Constructs</i>	27
<i>Transfection</i>	28
<i>Generating Mammary Organoids</i>	28
<i>HC11 and Primary Cell Organoid Analysis</i>	28
<i>Quantitative Real Time PCR Analysis</i>	29
<i>Whole Mount Production and Analysis</i>	29
<i>Mammary Epithelial Content Analysis</i>	29
<i>Mammary Lateral Branch Analysis</i>	30
<i>BrdU Incorporation Assay</i>	30
<i>Image Analysis and Quantification</i>	30
<i>Statistical Analysis</i>	30
Results.....	32
<i>Spy1 upregulation causes increased lateral side branching and mammary density</i>	32
<i>Spy1 increases mammary epithelial proliferation and secretion of AREG in the pubertal and adult mammary gland</i>	35
<i>Spy1 increases budding capacity in mammary epithelial cells</i>	38
<i>MMTV-Spy1 mouse primary cell organoids have higher budding capacity</i>	43
Discussion.....	47
Future Experiments.....	51
REFERENCES/BIBLIOGRAPHY	53
APPENDICES	64
Appendix 1 Protocols.....	64
Primary Cell Isolation Protocol.....	64
Permission.....	65

.....	65
VITA AUCTORIS	66

LIST OF TABLES

Table 1. **Mammary cell types**.....11

LIST OF FIGURES

Figure 1: Overview of mammary development	4
Figure 2: Schematic of branching models	8
Figure 3: Whole Mount analysis of Control versus MMTV-Spy1 glands during puberty	31-33
Figure 4: MMTV-Spy1 mammary glands have higher proliferation and AREG levels	36
Figure 5: Schematic of organoid preparation and production	38
Figure 6: Spy1 up-regulated HC11 Organoids have higher rates of budding	41
Figure 7: MMTV-Spy1 primary cell organoids have more growth and branching <i>invitro</i>	44
Supplementary Figure 1: Extended immunofluorescence channels for Spy1 and BrdU	38

LIST OF APPENDICES

Appendix 1 Protocols.....64

LIST OF ABBREVIATIONS/SYMBOLS

AREG.....	Amphiregulin
MMP.....	Matrix Metallo-Protease
MaSC.....	Mammary Stem Cell
TGF- β	Transforming Growth Factor β
EGFR.....	Epithelial Growth Factor Receptor
LTGF-beta.....	Lateral Transforming Growth Factor
TIMP.....	Tissue inhibitor of Metallo-Protease
DAB	3,3'-Diaminobenzidine
CAK	CDK activating kinase
CDK	Cyclin dependent kinase
CKI	Cyclin dependent kinase inhibitor
TEB.....	Terminal end Bud
FGF.....	Fibroblast Growth Factor
EGF.....	Epithelial Growth Factor
Stat.....	Signal Transducer and Activator of Transcription
Jak.....	Janus Kinase
DNA.....	Deoxyribonucleic acid
MMTV.....	Mouse Mammary Tumor Virus
BrdU.....	5-bromo-2'-deoxyuridine
Spy1.....	Speedy/RINGO Cell Cycle Regulator Family Member A
Ringo.....	Rapid Inducer of G2/M Progression in Oocytes A

FGFR.....Fibroblast Growth Factor Receptor
WNT.....Wingless-related integration site
RPMI.....Roswell Park Memorial Institute medium
PTEN.....Phosphatase and Tensin Homolog

Introduction

The Mammary Gland

The mammary gland is a secretory exocrine organ that follows a complex developmental history which leads to the eventual production of milk (Watson and Khaled, 2008). The term mammal comes from the Latin “mammās” or breast as all mammals possess mammary glands. The mammary gland is a functional organ exclusive to higher vertebrates which plays a key role in offspring development and survival and plays an important role in the life history of humans (Ofstedal, 2002). The development of the mammary gland is also linked to prevailing illnesses associated with the organ such as cancer (Nwabo Kamdje et al., 2017)

Most of mammary development occurs postnatally, which allows for genetic manipulation without the fear of consequences to other organs systems. Organ systems that develop in embryogenesis are often controlled by master regulatory genes that, when manipulated, can have effects on other organs or simply be lethal to the embryo. Therefore the mammary gland is an ideal study system. (Hens and Wysolmerski, 2005; Richert et al., 2000). Development of the post-embryonic mammary gland is characterized by epithelial invasion into the rudimentary fat-pad via ductal elongation until the ducts reach the end of the fat pad (Hinck and Silberstein, 2005). During puberty and progression into the adult gland there is an increase in secondary and tertiary side branching off previously formed ducts. During pregnancy, changes to the systemic hormone profile, such as an increase in estrogen and progesterone, have dramatic effects on the mammary gland (Vonderhaar and Greco, 1979). In this phase the mammary gland undergoes a spike in proliferation and a loss in adipocyte content; these changes allow for the eventual filling of the mammary gland and differentiation to produce alveoli. During lactation the mammary alveoli, the functional units of the gland which contain milk-producing cells and contractile cells, produce and distribute milk to the ducts as well as to the nipple (Watson and Khaled, 2008). Finally, following weaning, the mammary gland undergoes involution, an apoptotic period that returns the differentiated mammary gland to its resting state of development (Watson, 2006a).

As a model, the mouse mammary gland bears meaningful similarities to the human mammary gland in both structure, cellular composition, and development as well as cancer initiation

(Parmar and Cunha, 2004). The similarity of mouse mammary gland histology to human cancers is among the many reasons it serves as a viable model (Cardiff and Wellings, 1999). However, there are differences in morphology between the two species such as the epithelial functional units that extend the mammary gland. In mice stem cell rich structures called terminal end buds (TEBs) elongate the ductal structures further into the fat-pad. Conversely, the human ductal elongation is much more complex with 17-30 separate lobes connected to the nipple and formed through side branching of a primary duct. The functional unit of the human mammary gland is the terminal ductal lobular unit (TDLU) which bears similarities to TEBs in mice but whose cellular composition is not as well understood. Differences in the fat-pads of the two species include higher adipose cell content in the mouse, while the human fat-pad contains specialized stroma surrounding the TDLU's and rich in enzyme secreting fibroblasts (Dontu and Ince, 2015). Other differences include higher levels of involution in mouse versus human gland, and significantly lower baseline levels of estrogen in the mouse (Dontu and Ince, 2015). While it is important to highlight these differences when drawing comparisons, these discrepancies are outweighed by the similarities in the glands and utility of the mouse. Finally, the ability to manipulate gene expression that lead to different phenotypes and tumor susceptibility make the mouse mammary gland an ideal system to study developmental effects and tumor formation. (Hens and Wysolmerski, 2005).

Mouse Mammary Development in Embryogenesis and Puberty

Embryonic mammary gland development in the mouse begins during mid-gestation at embryonic day 10.5 (Cowin and Wysolmerski, 2010) where mammary lines form from the hindleg to the forelimb. At day 11.5, ectodermal cells situated on these mammary lines will migrate to 5 specific locations and aggregate to form a multilayered and column like placode (Cowin and Wysolmerski, 2010; Watson and Khaled, 2008). The cells within these mammary placodes differentiate to epithelial cells which are now distinct from their environment. Following this, at embryonic day 12.5 the mammary placodes become visible raised buds that begin invading downward into the dermal mesenchyme. At embryonic day 13.5 the buds invaginate entirely into the underlying mesenchyme to form the mammary buds (Briskin and O'Malley, 2010; Richert et al., 2000). The mesenchymal cells around the invaginated buds aggregate and form the mammary mesenchyme

(Richert et al., 2000; Watson and Khaled, 2008). During embryonic day 15 to 16 the mammary buds invade into the fat pad precursor and form a rudimentary ductal structure. Ductal development and branching are arrested at embryonic day 18.5 until estrogen-driven pubertal development occurs (Richert et al., 2000). In contrast to embryonic development, which is hormone-independent, growth during puberty occurs in a hormone-dependent manner (Briskin and O'Malley, 2010). At the onset of puberty, rapid, estrogen-driven proliferation and elongation of the duct drives development further into the mammary fat pad. Estrogen-driven growth leads to elongation of the rudimentary ductal tree until the leading edge of the duct reaches the end of the fat-pad. Ductal elongation is facilitated by the formation of terminal end buds or TEBs (Hinck and Silberstein, 2005; Richert et al., 2000) which invade and grow into the fat-pad. Terminal end buds are proliferative structures at the ends of the ducts which are formed by pluripotent stem-like cap cells that can divide rapidly and differentiate to the multitude of mammary cells known to constitute the gland. Cap cells that divide asymmetrically can differentiate into myoepithelial cells, which will line the outside of the elongating duct maintaining a direct connection to the surrounding stroma, or luminal epithelial cells which line the inside of the developing duct (Anderson et al., 2007; Richert et al., 2000; Watson and Khaled, 2008). Beneath the cap cells lie a multitude of dividing epithelial cells needed to move the gland forward by maintaining the structure of the developing duct. These epithelial cells will eventually undergo apoptosis and be degraded by macrophages to allow for hollowing of the duct, a process necessary for future differentiation and milk production (Briskin and O'Malley, 2010; Nelson et al., 2006; Richert et al., 2000). As TEBs invade into the fat-pad to extend the length of the developing duct, they bifurcate to produce new ductal branches of the primary line (Anderson et al., 2007; Hinck and Silberstein, 2005). Bifurcation is a well-regulated process and under the control of remodeling matrix metallo-proteases (MMPs) (Anderson et al., 2007). Once the TEBs reach the end of the fat-pad, around 8 to 12 weeks, they atrophy and become terminal ducts. A schematic of mammary development to the adult virgin can be seen in Figure 1. Estrogen and progesterone driven growth of side branches will continue in cycles unless pregnancy occurs.

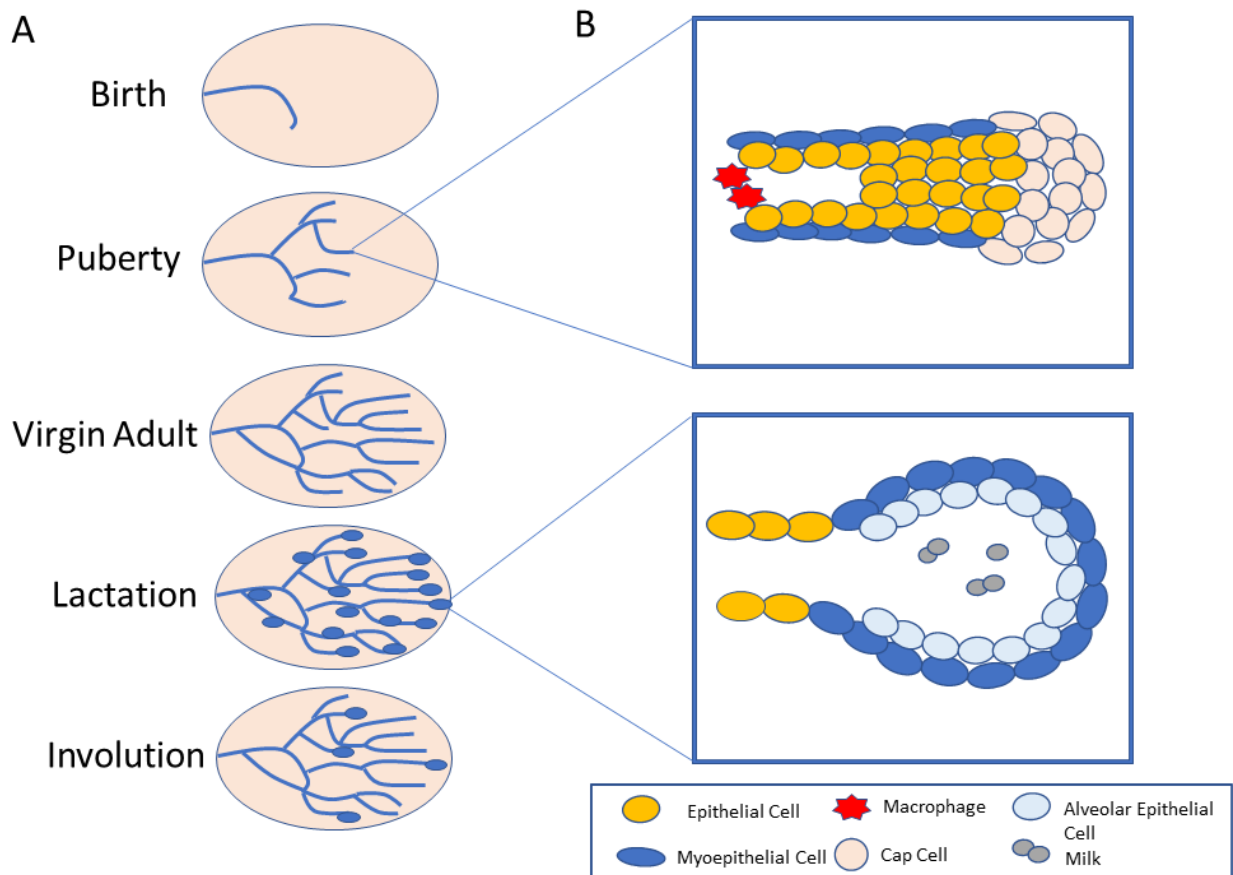


Figure 1. **Overview of mammary development.** A) Mammary development from birth to adult virgin. Embryonic mammary development leads to a rudimentary mammary tree which remains quiescent in the fat-pad until puberty. Pubertal increase in estrogen gives rise to TEBs at the ends of major ducts which proliferate and extend the mammary ductal tree towards the ends of the fat-pad. As the ducts extend unidirectionally, lateral branching works to fill the fat-pad in a multidirectional way and add unique patterning. This process continues until the mouse reaches adulthood or until pregnancy. During pregnancy estrogen and progesterone increase and tissue remodeling leads to alveoli formation for milk production. Lactation in the mouse mammary gland functions through alveolar epithelial cells producing milk and surrounding myoepithelial cells contracting and pushing it through the ducts back to the nipple. Once suckling stimuli are removed the gland is apoptotic-ally remodeled in involution back to the adult gland structure. B) Cell morphology of terminal end buds (TEBs) and lactating alveoli respectively. Figure adapted from (Inman et al., 2015).

Branching Morphogenesis and Lateral Branching

Branching morphogenesis is a process by which organ systems grow and develop the unique and functional properties of their architecture (Iber and Menshykau, 2013). It is a complex process by which a ductal network expands, filling the mesenchyme pad multi-directionally. Branching can occur in four major directional process: lateral branching, trilobed bifurcation, planar bifurcation and finally orthogonal bifurcation (Iber and Menshykau, 2013). A schematic of the four branching types can be seen in Figure 2. In many organ systems, the interplay between fibroblast growth factor 10 (FGF10) and sonic hedgehog (SHH) signaling is a key initiator and directional driver of bifurcation and branching. In the mouse lung, for example, the presence of FGF10 in the mesenchyme activates the fibroblast growth factor receptor (FGFR) in the local epithelial cells and upregulates proliferation while activating SHH signal (Bellusci et al., 1997). However, the salivary gland uses the same mesenchyme FGF10 epithelial receptor interplay but leads to SHH inhibition because the SHH-receptor complex acts in an inhibitory fashion in this organ system (Bellusci et al., 1997; Makarenkova et al., 2009). For a branching organ to achieve full arborization it requires symmetry-breaking events. These events are vital because simple tissue outgrowth will lead to rotational symmetry in the developing organ which cannot fully exploit the surrounding mesenchyme. As branching events extend epithelial tissue into the mesenchyme, they add an instability and unique patterning to the otherwise symmetrical outgrowth (Ochoa-Espinosa and Affolter, 2012) Symmetry breaking in a biological system is linked to increasing complexity and diversification which can give rise to specialized cellular structures with unique differentiation trajectories. In epithelial glandular cells, apical-basal polarity introduces a break in cellular symmetry that leads to two distinct epithelial surfaces – basal and often, luminal (Nelson, 2009). When this apical asymmetry is extended to whole tissues it gives rise to distinct organ functions. Other models have been explored to describe branching systems and the patterns they create. The mechanical branching model has been proposed to describe phenomena observed in tissue recombination systems; which used lung mesenchyme transplanted with ureteric epithelial buds leading to lung specific patterned growth in the kidney epithelium (Lin et al., 2001). The proposed mechanical model is based on differences in viscosity between the epithelium and mesenchyme where a process known as “viscous fingering” would produce branches from an expanding epithelium. While the authors admit the proposed model does not account for many aspects of

branching, together with signaling pathways and extra-cellular matrix inhibitory networks, the model could indeed play a role (Iber and Menshykau, 2013).

Interestingly, Hannezo et al proposed a unified model for branching morphogenesis that could account for the expansion of the mammary gland and branching using a simple mathematical rule set (Hannezo et al., 2017). The simulated model functioned on two major rules. The first rule is that an expanding duct can randomly choose between continuing to grow or bifurcating into two new units. The second rule was when an active tip reaches an already expanded duct it will terminate its growth and the branch will end. They demonstrated that this system alone, when limited to a simulated fat-pad, could effectively match the size and complexity of an adult mouse mammary ductal tree (Hannezo et al., 2017). Branching morphogenesis therefore likely involves several mechanisms including differences in signaling cascades, interplay between the mesenchyme and epithelium and inhibition based of proximity to growing and expanding ducts.

In the mouse mammary gland, ductal elongation and planar bifurcation are two of the main processes occurring during puberty that allow for expansion of the ductal tree. Lateral branching is a separate process that allows for further expansion of the ductal tree to fill the remainder of the fat pad. Initiation of lateral branch points occurs when increased proliferation at a specific point of the duct forms a mammary bud. Several paracrine and exocrine growth factors can elongate the mammary bud on their own once initiation has occurred (Moses and Barcellos-Hoff, 2011; Nelson et al., 2006). At specific locations along the developing mammary duct a decrease in Transforming Growth Factor- β (TGF- β), and an increase in levels of Fibroblast Growth Factor 2 (FGF2) and FGF10 as well as paracrine release of Epithelial Growth Factor (EGF) lead to formation of buds and subsequent formation of lateral branches, suggesting a similar feedback loop as the FGF10-FGFR SHH signaling pathway in other branching systems (Moses and Barcellos-Hoff, 2011; Nelson et al., 2006; Richert et al., 2000). TGF- β activation inhibits the formation of lateral branches throughout the duct. All cells are known to secrete LTGF- β , a TGF- β -1,3 precursor molecule, which can then be activated by a series of enzymes including matrix metallo-proteases (MMP) and integrins (Moses and Barcellos-Hoff, 2011). When activated, TGF- β and its accompanying receptor act as an inhibitory complex that is maintained at high levels in the developing duct. This consistent activation is needed to keep the duct from over-proliferating as it expands (Wakefield et al., 2001). When TGF- β -receptor I and II dimerize from TGF- β -1/3 signaling it leads to a cascade of events which activate Wnt5A, p16, p27 and finally the tumor suppressor p53. These factors

work to arrest the cell cycle through Cip/Kip family activation; which functions through p53 activation and inhibition of C-Myc, a regulator and proto-oncogene, that further inhibits proliferation (Aupperlee et al., 2013; Moses and Barcellos-Hoff, 2011). Forrester et al 2005 have also shown that mammary development can become hyperplastic and abnormal when TGF- β is knocked out, demonstrating its regulatory capacity in the developing duct (Forrester et al., 2005). Similarly, TGF- β -1 and TGF- β -3 were shown to have important and complex roles in several stages of mammary development by acting as inhibitors of tissue proliferation in the developing ducts, and as drivers of apoptosis and cell death in later involution stages (Moses and Barcellos-Hoff, 2011; Parvani et al., 2011). TGF- β activation has also been shown to decrease the number of basal cells in the mammary gland through ROBO1/SLIT signaling (Macias et al., 2011). SLITS are a conserved class of ligands that signal through ROBO receptors and guide axon formation and branching. In the mammary gland they have been shown to act as tumor suppressors by inhibiting canonical *Wnt* signaling (Marlow et al., 2008; Prasad et al., 2008). Furthermore, loss of SLIT/ROBO signaling leads to premature mammary branching (Macias et al., 2011). This inhibitory capacity of TGF- β is relevant to the developing mammary gland because it's a primary regulator of lateral branching in the developing duct through its ability to block local proliferation. Therefore, any changes to TGF- β or its downstream targets could change the degree and extent of lateral branching in mammary development.

The *Wnt* gene family play an important role in lateral side branching. Specifically, Wnt5A and Wnt5B signal non-canonically and inhibit branching morphogenesis and stem cell activation in the developing gland mammary gland (Roarty and Serra, 2007; Yu et al., 2016). *Wnt5a* is one of the downstream targets of TGF- β -1 activation (Wakefield et al., 2001) . Wnt5 activation is mediated through Ror2 receptor activation and sh-RNA deletion of Ror2 receptor leads to increased lateral side branching (Roarty et al., 2015). While non-canonical *Wnt* signaling has an inhibitory effect in the mammary gland, canonical *Wnt* signaling through *Wnt4* is needed for mammary regeneration in the luminal cell line (Yu et al., 2016). Indeed, Cai et al found that knockout of *Wnt4* and *Rspo1*, a *Wnt* family agonist, ablated the regenerative capacity of mammary cells when transplanted (Cai et al., 2014). The *Wnt* family plays important roles in all stages of mammary development from embryogenesis to ductal outgrowth is fundamentally required in lateral side branching (Brennan and Brown, 2004; Rajaram et al., 2015; Yu et al., 2016).

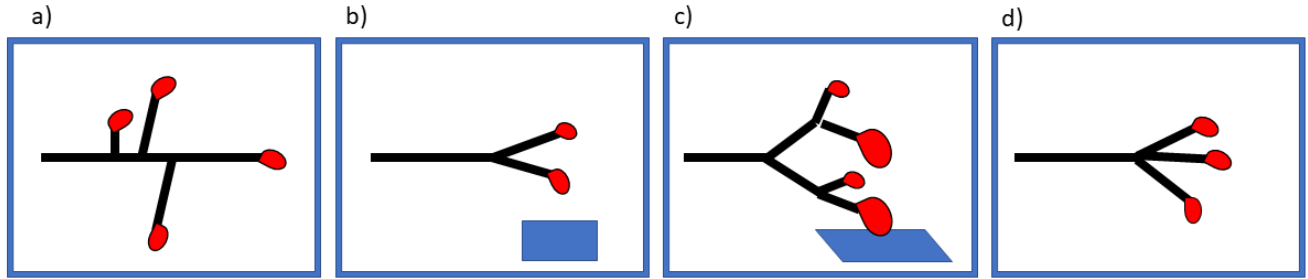


Figure 2. **Schematic of branching models:** a) lateral branching b) planar bifurcation c) orthogonal bifurcation d) trilobed/trifurcation (modified from (Iber and Menshykau, 2013) (Blue boxes represent 3-dimensional perspective of the growing buds with planar bifurcation growing in a flat plane and orthogonal bifurcation alternating between flat horizontal plane and vertical plane. Red tips represent the extending terminal end buds)

Molecular Signaling in Mammary Proliferation

One of the primary pathways used for growth in the mammary ductal tree is the estrogen-dependent amphiregulin (AREG) pathway (Sternlicht and Sunnarborg, 2008). This pathway is initiated by activation of estrogen receptor by ovarian estrogens; this leads to a cascading event that increases the production of membrane bound amphiregulin. Amphiregulin is then cleaved by the G-coupled protein ADAM-17 whereupon a released domain then moves to bind to Epidermal Growth Factor Receptor (EGFR) on the surface of a nearby stromal fibroblast. AREG may also bind to EGFR in a paracrine fashion on another epithelial cell (Aupperlee et al., 2013; Sternlicht and Sunnarborg, 2008). EGFR then dimerizes and induces the release of FGFs from the stromal cell into the stromal-epithelial cleft where they can then bind to the epithelial cells' FGFR. This paracrine process leads to local proliferation within the mammary gland (Aupperlee et al., 2013; Vonderhaar and Greco, 1979). EGFR ligand-activated proliferation is primarily relevant in puberty and early pregnancy because it aids in elongation of side branching and formation of budding (Aupperlee et al., 2013). This paracrine pathway is necessary in puberty due to the increase in lateral side branching and need to maintain the mammary architecture in the event of damage or change (Aupperlee et al., 2013; Vonderhaar and Greco, 1979).

Pregnancy and Lactation

The onset of pregnancy stimulates a change in the hormonal profile with increases in levels of estrogen and progesterone (Brisken and O'Malley, 2010; Richert et al., 2000). Once this switch is achieved, a sizeable increase in proliferation occurs in the mammary gland. This proliferation leads to increased side branching until the fat-pad is almost entirely filled with the ductal network (Richert et al., 2000). Following this, differentiation occurs wherein the ends of new and old ductal structures begin forming functional alveoli which will be the site of milk production (Oakes et al., 2006). Alveoli are bulbous structures composed of an inner luminal epithelial cell layer that becomes distended in late pregnancy, and an outer myoepithelial layer which is connected to the basement membrane. The inner epithelial cell layer produces milk when stimulated and secretes it into the lumen of the alveolus (Anderson et al., 2007; Oakes et al., 2006; Richert et al., 2000),

while the myoepithelial cells contract and push the milk into the duct. Another feature of the inner luminal layer is that it is interconnected by tight junctions while the cells are highly polarized. The cytoplasm of the inner epithelial cells mostly consists of endoplasmic reticula which aids in production and secretion of milk (Anderson et al., 2007). Milk production continues until weaning occurs and the pups no longer require milk. Restructuring of the mammary gland during pregnancy involves a decrease in the adipocyte ratio of the fat-pad. The adipocyte ratio is the percentage of adipocytes in the mammary gland as compared to the epithelium. Furthermore, this drop in the ratio is followed by expansion of the epithelial cell population. This decrease in the total number of adipocytes creates the room needed for alveolar development. While puberty is driven mainly by estrogen, pregnancy and lactation are under control of progesterone and prolactin respectively (Richert et al., 2000; Vonderhaar and Greco, 1979). Progesterone drives the increase in lateral branching that leads to filling of the fat pad as well as the differentiation and restructuring required to form alveoli. (Anderson et al., 2007; Hens and Wysolmerski, 2005). In Progesterone Isoform B negative mice lobuloalveolar development of the mammary gland is reduced, with lateral branching and alveolar development being significantly reduced through decreased proliferation and loss of epithelial content (Mulac-Jericevic et al., 2003). Prolactin is the primary driver of differentiation in the mammary gland and works through the Jak-Stat pathway (Hughes and Watson, 2012; Watson and Burdon, 1996). Pregnancy and lactation are stages of significant gland remodeling and differentiation which are needed for efficient milk production. The production of milk and state of lactation will continue until the suckling stimulus is removed, at which point the gland will be remodeled back to its pubertal state.

Involution

Involution is a stage of mammary development characterized by apoptosis and structural remodeling to revert the gland back to its pre-pregnant stage. Involution is triggered by removal of the suckling stimulus and accumulation of milk (Marti et al., 1997; Watson, 2006a). As involution begins, the secretory epithelial cells start to gain large vacuoles that contain fat droplets and casein protein. The presence of milk in the alveolar lumen triggers the expression of TGF- β -3 and leukemia death factor which activate Stat3 (Chapman et al., 2000; Hughes and Watson, 2012). Flanders et al has shown that TGF- β -3 is an initiator of apoptosis necessary for

triggering involution in the mouse mammary gland (Flanders and Wakefield, 2009). Enzymatic destruction of accumulated vacuoles and activation of Stat3 both lead to cell apoptosis in the luminal epithelium, debris and secretions are then subsequently shed into the alveolar lumen (Li et al., 1997; Watson, 2006a). The cells shed into the alveolar lumen are cleared by macrophages, that then begin aggregating towards the alveoli (O'Brien et al., 2012). The process is reversible up to 48 hours, at which point, restructuring of the gland occurs and the second irreversible stage of involution begins (Lund et al., 1996). The second stage of involution is marked by collapse of the alveoli and migration of adipocytes back into the fat-pad to differentiate into mature adipose tissue. MMPs play a significant role in the second irreversible stage of involution by breaking down the extra-cellular matrix around alveoli and activating Plasmin which allows for differentiation of adipocytes (C.H.Streuli, 1996; Green and Lund, 2005). MMPs are under tight regulatory control by Tissue Inhibitors of Metallo-Proteases (TIMPS) due to their importance in involution. In TIMP deficient mice, involution is accelerated and no longer reversible in the first stage due to faster activation of MMPs. As remodeling continues and epithelial cells are replaced by differentiating adipocytes, macrophages remove accumulated cell debris through phagocytosis (Green and Lund, 2005; Lund et al., 1996). The basement membrane and myoepithelial cells attached to it are preserved through survival signals activated by several hormonal cues (Li et al., 1997; Watson, 2006b). By day 21 of involution the gland has been remodeled back to its pre-pregnant stage, but it maintains a level of differentiation higher than that of virgin mice at similar ages. This process and the ability of mice to undergo continuous and cyclic development hints at the likelihood of stem cell progenitors within the mammary architecture (Richert et al., 2000).

Mammary Stem Cells in the Adult Gland

The adult mouse mammary gland is a heterogenous structure that contains several different cell types with different proliferative and differential capacities (Richert et al., 2000). All mammary cells are derived from the differentiation of totipotent fetal stem cells which then become common short term and long-term repopulating progenitor cells. These cells are characterized by their Estrogen- (ER⁻) and Progesterone Receptor (PR⁻) negative-status and are known to be multipotent (Visvader and Stingl, 2014). Serial dilution experiments have shown that one mammary stem cell can recapitulate the entire mammary gland in a cleared fat-pad (Visvader and

Stingl, 2014). This mammary stem cell population is characterized by staining for CD49^{hi} CD29^{hi} CD24^{+/mod} Sca1^{low} (Visvader and Lindeman, 2006; Visvader and Stingl, 2014). Characterization of cell populations by presence and absence of specific markers is valuable in determining cell types and their derivatives (citation). CD24, for example is a signal transducer glycoprotein known to modulate growth and its absence has been associated with aggressive mammary tumors ((Hilka et al., 2005)). Isolation of this population of cells is complicated by the fact that certain differentiated cells also express a similar surface marker expression profile (Visvader and Lindeman, 2006). Mammary stem cells (MaSCs) divide asymmetrically, one daughter cell remaining a MaSC while the other becomes a more differentiated cell. This process allows MaSCs to produce both types of progenitor lines, luminal and basal, while maintaining the original stem cell population. Asymmetric division is therefore necessary for maintenance of mammary stem cells and to preserve future capacity for a rapid expansion of progenitors, which can then quickly recapitulate any lost mature cells through symmetric division (Ercan et al., 2011; Visvader and Lindeman, 2006). It is proposed that long term- and short term-repopulating stem cells are able to differentiate into luminal lineage stem cells and basal lineage stem cells, which are multipotent and can give rise to their own progenitor populations. Quantifying and classifying different progenitor cell types in the mammary gland is difficult due in part to the fact that receptor staining is measured by relative abundance of certain markers rather than absolute presence or absence (Visvader and Lindeman, 2006). Myoepithelial progenitor cells proliferate symmetrically to rapidly produce differentiated and mature myoepithelial cells. Myoepithelial cells are basal cells that sit on the outside of the duct and behind luminal cells; they are in direct contact with the basement membrane resting closer to the fibroblast rich stroma and adipose rich fat pad exterior (Visvader and Lindeman, 2006). Myoepithelial cells also play a functional role in lactation by contracting and helping push the milk inside the lumen of the alveolus into the duct. These cells can be visualized by staining for specific markers such as CD29^{hi} CD49^{hi} CD24⁺ EpCAM^{lo/med} (Visvader and Lindeman, 2006; Visvader and Stingl, 2014). The luminal epithelial lineages have two known progenitors that both rapidly divide to replenish their mature progeny. The luminal cell lineage has a proposed common progenitor stem cell line that can asymmetrically produce a ductal progenitor and early alveolar progenitor luminal cell which can be stained with CD49⁺ CD29^{lo} CD24⁺ /hiepCAM^{hi} CD61c-kitSca1⁺ CD49b⁺ CD14⁺ and CD49⁺ CD29^{lo} CD24⁺ /hiepCAM^{hi} CD61c-kitSca1-CD49b⁺ CD14⁺ ALDH⁺ respectively (Visvader and Lindeman, 2006; Visvader and Stingl, 2014). Ductal progenitor cells divide and differentiate directly into mature ductal luminal cells which lines the inside of the

mature mammary ducts and secretes extra cellular matrix necessary for the integrity of the ductal structure. (Shehata et al., 2012). The mature ductal cells possess markers CD49^{fl}CD29^{lo}CD24⁺CD14⁻epCAM^{hi}kit⁻Sca1⁺CD61⁻CD49b⁻ (Visvader and Lindeman, 2006; Visvader and Stingl, 2014). The plasticity and heterogenous nature of the mouse mammary gland is largely responsible for why this organ is capable of continuous development throughout the lifecycle of the animal.

Cell Type	Staining Markers
Mammary Stem Cell	CD49 ^{hi} CD29 ^{hi} CD24 ^{+/mod} Sca1 ^{low}
Ductal Progenitor Cell	CD49 ^{f*} CD29 ^{lo} CD24 ^{+/hi} epCAM ^{hi} CD61 ^{c-} kit ^{Sca1⁺ CD49b⁺ CD14⁺}
Early Alveolar Progenitor Cells	CD49 ^{f*} CD29 ^{lo} CD24 ^{+/hi} epCAM ^{hi} CD61 ^{c-} kit ^{Sca1⁻ CD49b⁺ CD14⁺ ALDH⁺}
Myoepithelial Cell	CD29 ^{hi} CD49 ^{hi} CD24 ⁺ EpCAM _{lo/med}
Ductal Epithelial Cell	CD49 ^{fl} CD29 ^{lo} CD24 ⁺ CD14 ⁻ epCAM ^{hi} kit ⁻ Sca1 ⁺ CD61 ⁻ CD49b ⁻
Ductal Alveolar Cell	CD49 ^{f*} CD29 ^{lo} CD24 ^{+/hi} epCAM ^{hi} CD61 ^{c-} kit ^{Sca1⁻ CD49b⁺ CD14⁺ ALDH⁺}

Table 1 **Mammary Cell Types**. Cell types present in the mammary gland and their respective staining markers.

Tumor Susceptibility and Abnormal Mammary Development

Due to the nature of mammary development and the complexity inherent in all its stages, there are many time points where mammary gland development can be mis-regulated. In general, abnormal organ development leads to susceptibility to illness, both cancer and otherwise; the mammary gland is no exception to this rule (Ercan et al., 2011; Veltmaat et al., 2013). Epidemiological studies in adolescent girls have found that pubertal development is a significant time point for increased susceptibility to breast cancer and tumorigenesis (Biro and Deardorff, 2013; Bodicoat et al., 2014; Johnson et al., 2013). The reason for this is that pubertal development activates a series of hormonal and adrenal pathways that lead to proliferation and changes in structure and morphology of the gland (Briskin and O'Malley, 2010; Richert et al., 2000; Saji et al., 2000). Dysregulation in the balance of proliferation and expansion of the known stem cell populations in puberty can be one transition to tumorigenesis due simply to hyperplasia and eventual neoplasia (Bodicoat et al., 2014; Ercan et al., 2011). Increased proliferation requires DNA synthesis and subsequent cell division which are under the control of cell cycle regulators and tumor suppressors such as *BRCA1* and *BRCA2* or *PTEN* (Narod and Salmena, 2011; Shore et al., 2016). When tumor suppressors that limit DNA damage by arresting the cell cycle are mutated or mis-regulated any increase in proliferation can increase the potential for mutations and initiation of breast cancer. Once an initiating event has occurred most cancers will often have a latency period. A latency period is the time that the tumor is establishing itself in the tissue and has no physiological effects. During latency period the tumor may vascularize and transition through its multiple stages of aggressiveness. The latency period ends when a diagnosis is made, which can be multiple years after the initiating event and at multiple stages. Therefore, modelling latency periods can give insight into appropriate screening times as susceptibility to cancer increases with age (Olsson et al., 2003). While rarer, breast cancers among young women were found to be more aggressive with poorer prognosis than those found among women over 40 (Johnson et al., 2013). In mice, as in humans, a susceptibility window for tumorigenesis and breast cancer exists during puberty. Gang Li et al 2002 found that when *PTEN*, a known tumor suppressor, is knocked out in the mammary gland, the gland fails to differentiate properly and begins to hyper-proliferate (Li et al., 2002). This increase in proliferation and poor differentiation are accompanied by increased side branching and ductal elongation and finally tumor formation. This study perfectly demonstrates the transition from hyperplasia to neoplasia. Shore et al shows that when *PTEN* is

knocked out of only luminal epithelial cells the gland has transient developmental effects (Shore et al., 2016). A loss of polarity and a failure in proper distribution of luminal cells accompanied by disrupted mammary architecture in the mature gland are two of the primary effects seen (Shore et al., 2016). Proper mammary development is therefore an essential process in maintaining a functional adult mammary gland and avoiding cancer (Moser et al.; Russo et al., 1979).

The Cell Cycle

The cell cycle is complex system of phases, checkpoints and proteins that allow a cell to divide. It serves a fundamental role as the primary and interconnected system needed for any cellular reproduction (Schafer, 1998; Teyssier et al., 1999). The cell cycle consists of four primary stages: G1, S, G2 and M. G1 stands for the Gap1 stage during which growth and total cell content increases (Cowin and Wysolmerski, 2010; Schafer, 1998). If there are any cellular imperfections or damage the cell is arrested in G1 by specific checkpoint proteins known as cell cycle inhibitors or CKIs (Schafer, 1998). Nakayama et al. found that when certain checkpoint proteins, such as a Kip1 family member, are knocked out, the cell cycle progresses haphazardly leading to organ hyperplasia and pituitary tumors (Nakayama et al., 1996). After G1 cells enter the synthesis or S phase, DNA replicates rapidly in anticipation for cell division. Cells then enter the final gap phase of G2; cells undergo more growth and protein synthesis until the appropriate size is reached for them to divide. As cells wait in G2 there is an increase in phosphorylated checkpoint kinases. This accumulation of phosphorylated checkpoint kinase complexes is the key determining factor in G2 that will lead the phase transition to M (Porter and Donoghue, 2003). The final phase is mitosis or M phase which culminates in the separation of two identical daughter cells, each with their own copy of the parent DNA. Finally G0 is a unique stage of the cell cycle that effectively removes the cell from continuous replication (Barnum and O'Connell, 2014). This process was originally thought to occur in cells that were nutrient deprived or otherwise under stress and was therefore coined as a resting phase. G0 is now better understood as its own specific stage outside the classic cell cycle that has important functions in many organ systems. The G0 stage can be either reversible or irreversible depending on the cell type and reason for entering (Rodgers et al., 2014). Reversible G0 is known as quiescence, a state that stem cells will often sit in until cues from local cell types drive them to re-enter the cell cycle and proliferate. Irreversible G0 states include both

senescence and differentiation where cells such as mature neurons or terminally differentiated mammary fibroblasts can no longer divide, but instead provide functional roles to local architecture (Harashima et al., 2013).

CDKs, Cyclins and CKIs

The cell cycle and its drivers require complex and intricate checkpoints, otherwise cell division could easily spiral into increased proliferation which can lead to genomic instability (Malumbres and Barbacid, 2009). Cyclin dependent kinases (CDKs) are a class of serine-threonine kinases that play vital roles in the cell cycle (Schafer, 1998). CDKs are vital due to their ability to phosphorylate and activate a large array of proteins involved in the intricate steps and decisions of cell division (Malumbres and Barbacid, 2009). Subsequently, these cascading signaling events activate DNA which then encode protein products that allow for progress past cell cycle checkpoints. There are 8 total CDKs that have been characterized with 4 of them being the most well characterized. These are CDK1, CDK2, CDK4 and CDK6 (Schafer, 1998). Cyclins are a class of proteins that act as co-activators of CDKs (Harashima et al., 2013; Noble and Endicott, 2001). Cyclins were discovered after CDKs (Jackson, 2008). There are a variety of known cyclins, each with their own semi-specific CDK binding partner and time point of high abundance in the cell cycle (Harashima et al., 2013; Noble and Endicott, 2001). CDK expression remains constant during the progression of the cell cycle, while cyclins shift in their production and degradation depending on the stage of the cell cycle (Harashima et al., 2013). For example, the transition between G1 to S is under the regulatory control of the CDK2-CyclinE complex which phosphorylates target proteins specific for transition to S phase. The transition from G2 to M is similarly under the control of the CDK1-CyclinB complex which determines when the transition from G2 to M occurs. Similarly, CDK4 and 6 are responsible for moving the cell cycle through the early stages of G1 to S while also having the ability to arrest the cell cycle if the conditions for cell cycle progression are not ideal; these conditions being nutrient availability, cell damage and environmental conditions (Borel et al., 2002).

The balance of CDK-cyclin complex activation is complex and highly regulated by a variety of genes (Barnum and O'Connell, 2014; Harashima et al., 2013; Schafer, 1998). All CDKs are defined by having a cyclin binding P-STAIRE domain in the C-terminus. This domain is an ATP-binding catalytic

cleft and a catalytic site obstructing T-loop motif (Lim and Kaldis, 2013). CDKs are activated by cyclins through a two step process which first involves binding of the cyclin to the P-STAIR domain of the CDKs. This first step leads to a conformational change that exposes the T-loop by pulling it off the active site and flattening it towards the cyclin, which allows the CDK to be phosphorylated and activated. During step two, phosphorylation of the CDK by CDK activating kinases (CAKs) occurs on a threonine residue of the T-loop close to the catalytic site, which now fully activates the CDK and allows it to phosphorylate its own targets. In the specific case of CDK2, activation occurs when threonine 160 of the T-loop is phosphorylated which flattens the T-loop and brings it close sterically to the cyclin (Malumbres, 2014). This post-translation change opens the catalytic site of CDK2 which maintains a binding preference for S/T-P-X-K/R consensus sequences (Malumbres, 2014; Martinez et al., 1997). Furthermore, while this preference accommodates prolines in position 1 but it is far less stringent in position 3. (Noble and Endicott, 2001). CDK inhibitors (CKIs) are a family of proteins that can inhibit either the CDKs directly or CDK-Cyclin complexes to arrest the cell cycle during its respective phase. The INK4 family of proteins, which includes: p15, p16, p18, p19, are all capable of targeting CDK4/6 and arresting the cell cycle in G1 (Cánepa et al., 2007). The second family of CDK inhibitors is the Cip/Kip family consisting of: p27, p21 and p57 (Nakayama and Nakayama, 1998; Querada et al., 2016). The Cip/Kip family can inhibit Cyclin-CDK complexes by obstructing a substrate binding domain on the cyclin subunit called the MRAIL motif and subsequently binding to the catalytic cleft of the CDK thereby inhibiting ATP binding (Besson et al., 2008). In mammals the Cip/Kip family primarily targets CDK2 and its binding partners cyclin A and E (Denicourt and Dowdy, 2004). While arresting the cell cycle is the primary role of CKIs, they can also stabilize and aid in the binding of some 11 CDKs to their cyclins, such as the stabilizing effect p27 has on CDK4/6 binding to Cyclin D (Denicourt and Dowdy, 2004). Therefore, CKIs play a very vital role in the regulation of the cell cycle. p27 specifically, is involved in arresting the cell cycle indefinitely in circumstances of cell aging, (Barnum and O'Connell, 2014; Flores et al., 2014; Malumbres and Barbacid, 2009).

SPDYA/Spy1

Spy1 is a cyclin-like protein that drives the cell cycle and overrides specific cell cycle checkpoints, such as the Cip/Kip family. Also known as X-Spy1 or Ringo, the Spy1 protein was originally

discovered in a screen of a *Xenopus laevis* cDNA library in a *rad1* deficient strain of *S.Pombe*. The objective was to find cDNAs that encoded factors that would help this genetically deficient yeast line to recover from UV radiation damage (Lenormand et al., 1999). Rad1 is a checkpoint DNA repair protein that combined with Rad10 can form an endonuclease capable of degrading single stranded DNA. Furthermore, in the event of DNA damage Rad1 is needed for the yeast to transition past the G2/M checkpoint as it functions to repair DNA. (Schiestl and Prakash, 1988; Tomkinson et al., 1993). With a deficiency in *rad1* damaged arrest at the G2/M checkpoint, an effect that will be lethal if the DNA is not repaired. A *Xenopus laevis* cDNA library was used to identify genes that were able to push past the checkpoint and confer resistance to DNA damage. *Xenopus-Spy1* (X-Spy1) was isolated due to its ability to drive the cell cycle past the G2/M checkpoint even in the event of DNA damage. (Lenormand et al., 1999; Nebreda and Hunt, 1993). In *Xenopus*, oocyte maturation is a two-step process with the first step arresting oocytes in G2/M at the first meiotic division. In the presence of progesterone, the cell cycle continues, and oocytes enter meiosis I and are arrested again at M stage of meiosis II until fertilization (Lenormand et al., 1999) The labs of Dr. Angel Nebreda and Dr. Donoghue also found that X-Spy1 could activate CDK1 to drive the cell cycle forward in G2 arrested *Xenopus* oocytes when its primary driving hormone progesterone was absent (Ferby et al., 1999; Lenormand et al., 1999). Interestingly, it was also found that when X-Spy1, known also as p33RINGO, was silenced using antisense oligonucleotides the oocytes were delayed in their maturation, even after induction with progesterone (Ferby et al., 1999). This data led researchers to conclude that X-Spy1 played a role in *Xenopus* oocyte maturation and subsequent release from G2 block. It was also found that X-Spy1 had no sequence homology with known cyclins and CDK activators but can activate CDK2 in the process of oocyte maturation. (Karaiskou et al., 2001; Lenormand et al., 1999). Through studies focusing on deletion mutants of X-Spy1 it was found that amino acids 54-218 constitute a functional "Speedy/Ringo box (S/R box)" which is necessary for its binding to CDKs. The human clone of SPY1 was isolated using testis cDNA library focused on identifying genes with high homology to X-Spy1 (McGrath et al., 2017). The human homologue of X-Spy1, SPDYA had 40% homology to X-Spy1 and over 60% homology for its functional central region. To test if the human homologue of X-Spy1 has the same functional properties, mRNA of human Spy1(SPY1) was injected into *Xenopus* oocytes and found to induce G2/M transition therefore confirming that the homology is functional (Barnes et al., 2003; Porter et al., 2002). There are at least six known mammalian Spy1/Ringo homologues all sharing around 50% homology within the S/R box (Cheng

et al., 2005a; Dinarina et al., 2005). There have been no homologues of Spy1 identified in yeast, worms, flies or plants. In humans, Spy1 is expressed in a variety of tissues. (Barnes et al., 2003; Cheng et al., 2005a). Further investigation into human Spy1 revealed 5 family members of the Spy1/Ringo family, with the original characterized Spy1 being Speedy/Ringo A. Spy1/Ringo A was shown to have two isoforms, Speedy/Ringo A1 and A2. Spy1A1 was found to be identical to the originally identified human SPY1 and will be referred simply as Spy1 from here on (Cheng et al., 2005b; Porter et al., 2002). Upregulation of Spy1 in cell lines leads to increased proliferation and activation of CDK2 at the G1/S checkpoint (Porter et al., 2002). Furthermore, inhibition of CDK2 negated the effect of Spy1 upregulation thereby demonstrating its effect as a binding partner (McAndrew et al., 2009). Unlike traditional cyclin binding mechanisms, Spy1 activation of CDKs is functionally unique. Traditional CDK activation begins with cyclins binding to the CDK and inducing a conformational change by exposing the T-loop and pulling it off the catalytic cleft. The T-loop is then typically phosphorylated on a threonine residue near the CDK active site and the flattened conformational change away from the catalytic site is maintained which fully activates the CDK (Barnum and O'Connell, 2014). Spy1 can activate CDKs by binding and changing the conformation so that T-loop phosphorylation is unnecessary for full activation and localization of the CDK (Cheng et al., 2005b; McGrath et al., 2017; Porter et al., 2002). In characterizing the 3D structure of Spy1 McGrath et al showed that the CDK2 T-loop was moved 5-6 Angstroms (Å) off the catalytic cleft when bound to Spy1 (McGrath et al., 2017). Furthermore, Spy1 subunit T136 was found to be bound to CDK2 T-loop Threonine 160 and subunits D97 and T134 were bound to CDK2's T158 and D159 which are typically sterically inaccessible in an inactive CDK. In comparison to cyclin A, Spy1 formed several unique binding interactions with CDK2 which likely facilitate its ability to expose the catalytic site and coordinate the CDK (McGrath et al., 2017). This effect of Spy1 was also demonstrated when Cheng et al. showed CDKs with mutated Thr160 and Thr161 residues were activated in the presence of Spy1 (Cheng et al., 2005b). The reason for Spy1's ability to activate CDKs in a non-traditional manner, even though its binding patterns are not unique, is due to the conformation change it induces in the target CDKs bound (Cheng et al., 2005b; Karaïskou et al., 2001; McGrath et al., 2017).

Spy1 is also unique to other cyclins through its interaction with CKIs. CKIs play important roles in regulating the cell cycle and arresting it at specific checkpoints. Spy1 activation of CDK2 has been shown to be less susceptible to inhibition by p21, a member of the G1 arresting Cip/Kip family (McAndrew et al., 2009). Furthermore, Spy1 has been shown to interact with p27, another

member of the Cip/Kip family, and to increase its turnover rate in the G1/S phase. Spy1 increases the turnover of p27 through phosphorylation on its Th187 residue, consequently targeting it for degradation (Al Sorkhy et al., 2016; McGrath et al., 2017). Sorkhy et al also demonstrated that a p27 inhibitory interaction with CDK2-Cyclin complex was weaker when bound to Spy1. This could be due to Spy1 lacking a hydrophobic binding motif found on many cyclins called the MRAIL site (McGrath et al., 2017). Collectively, Spy1 is a versatile driver of the cell cycle due to its ability to activate CDKs independent of phosphorylation and degrade and negate the effects of CKIs.

The expression of Spy1 is under tight regulatory control by a class of proteins known as ubiquitin ligases. E3 Ubiquitin ligases are proteins that can attach multiple small regulatory ubiquitin proteins to their targets and mark them for degradation by the proteasome. Furthermore, the proteins known as “ubiquitin ligase neural precursor cell expressed developmentally down-regulated protein 4” and the “Skp, Cullin F-box containing complex” (Nedd4 and SCF) are two proteins which control the levels of Spy1 through degradation (Sorkhy et al., 2009). The SCF complex is a E3 ubiquitin ligase that drives the cell cycle by poly-ubiquitinating CKIs and marking them for proteasomal degradation. It targets Cip/Kip family members p27 and p21 specifically as well as Cyclin E. Dinarina et al. showed that in non-synchronous cells, SCF inhibition, but not the anaphase promoting complex (APC/C), will lead to accumulation of Spy1 (Dinarina et al., 2009). The other known Spy1 inhibiting ubiquitin ligase NEDD4 is a widely expressed regulator shown to be vital in neural morphology and organ development (Cao et al., 2008). Through co-immuno precipitation NEDD4 was shown to interact with Spy1 in-vivo. Furthermore, Spy1 ubiquitination was significantly decreased in the presence of ubiquitin non-binding dominant negative mutant of NEDD4 (Sorkhy et al., 2009). In contrast to X-Spy1 human Spy1 degradation requires phosphorylation on its N-terminal domain with the C-terminus being dispensable (Sorkhy et al., 2009). Spy1 abundance was shown to be proteasome-dependent with lack of N-terminal ubiquitination leading to higher protein stability (Sorkhy et al., 2009). Due to Spy1’s myriad of effects, its expression in the developing mammary gland is therefore likely very important as mis-regulation could have a variety of consequences on the morphology of the gland.

Spy1 and Mammary Development

Endogenous expression of Spy1 in the developing mammary gland follows a cyclic trend and correlates with periods of development characterized by increased proliferation and apoptosis (Golipour et al., 2008). Spy1 is highly expressed during early stages of development such as pre-pubescent growth all the way into early pregnancy. The levels of Spy1 start to decrease during late pregnancy and into lactation as the gland differentiates and develops functional alveoli (Al Sorkhy et al., 2012; Golipour et al., 2008). Decrease in Spy1 abundance during differentiation was confirmed both with a time-course study and by using HC11 cells as a model system. HC11 cells are an immortalized mammary epithelial cell line that responds to similar cues *in-vitro* as would lead to differentiation or proliferation *in-vivo* (Ball et al., 1988). Golipour et al found that when Spy1 is overexpressed during differentiation in HC11 cells there is earlier expression of β -casein, a milk protein known to delineate differentiation in mammary development (Golipour et al., 2008). During involution Spy1 levels begin to rise again until reaching levels in the adult gland (Golipour et al., 2008). It was also found that when fat-pad transplants are done with Spy1 overexpression in HC11 cells into the cleared glands of 3-week-old mice, the glands show increased staining with markers such as PCNA as well as hyperplasia and disruption of mammary architecture (Golipour et al., 2008). Spy1 up-regulated cells grow in a disorganized fashion with loss of polarity and apical linearity (Golipour et al., 2008). Spy1 regulates the ER- α and ERK1/2 pathways to promote resistance to anti-estrogen chemotherapeutic tamoxifen (Ferraiuolo et al., 2017). Elevated Spy1 levels were found in many types of aggressive human breast cancers, specifically triple-negative and Her2 negative breast cancers (Al Sorkhy et al., 2012). When using a non-degradable Spy1-TST mutant (developed with alanine mutations at Tyrosine 15 Serine 22 and Tyrosine 33), Al Sorkhy et al. found increased likelihood of tumorigenesis demonstrating the importance of Spy1 in possible breast cancer initiation (Al Sorkhy et al., 2012). With all the evidence showing the effects of Spy1 expression in the mammary gland and its potential initiating capacity in tumorigenesis it's likely that Spy1 serves important functional roles both in mammary development and maintenance. Therefore, further elucidation of its roles and the pathways it affects is required.

Transgenic Mouse Models

Transgenic animal models are a cornerstone development of modern molecular biology (Haruyama et al., 2009). There is no shortage of pathways, phenotypes or conditions that can be investigated using transgenic mouse models. The development of transgenic models in the early 1970s ushered in the modern application seen today in genetics, cancer and developmental studies (Doyle et al., 2012). The first transgenic mouse was developed using pro-nuclear injections. Pronuclear injections insert a DNA construct directly into the recently fertilized mouse egg, while the maternal and paternal DNA are still separate. Pronuclear injections cannot guarantee the location of gene insertion or the number of gene inserts. Using this technique, the first transgenic mouse was developed in the 1980s by Dr. Jon W Gordon (Gordon et al., 1980). While unsuccessful in expressing the gene in question, the breakthrough did lead to the first mouse with a visible phenotype from pronuclear injection (Doyle et al., 2012; Hanahan et al., 2007; Haruyama et al., 2009; Jones, 2011). The technique was then refined over time and injection of double stranded DNA encoding the gene in question within a vector to drive its expression using endogenous housekeeping genes was developed. An example of this would be a transgenic mouse with the aim of expressing its transgene constitutively in alveolar type 2 cells would utilize a surfactant protein C promoter. (Doyle et al., 2012; Haruyama et al., 2009). Eventually the development of inducible gene expression was developed wherein a gene in question is under the control of an activated promoter, such as human Cytomegalovirus promoter (Schottstedt et al., 2010); this system allows for the gene to be expressed transiently or at specific time-points in the lifecycle of the organism (Doyle et al., 2012; Sun et al., 2007).

While transgenic animal models are useful in the field of molecular biology they do come with certain drawbacks. Firstly, the inserted DNA must be injected into the pronucleus before the first cleavage of the zygote (Doyle et al., 2012). If the first cleavage occurs and DNA begins to double in the organism before the DNA of interest can be inserted, the animal will be a genetic (and presumably phenotypic) mosaic. Furthermore, the gene in question inserts randomly into the host DNA with a variable copy number which could lead to phenotypic effects arising from disruption of local context at the insertion site. Moreover, the copy number of inserted genes could lead to non-specific or unintended gene dosage effects. DNA insertion into a proto-oncogenes or other vital regulatory gene families disrupting their function can result in cancer

and morphological defects (Ikink et al., 2018). Multiple insertions do not necessarily mean significant increase in the transcription of the gene so analysis of gene transcription as a confirmation is always necessary (Gordon et al., 1980; Liu, 2013). Finally, if the gene is inserted into a heterochromatic region of the chromosome then its effects will be negated by the inhibitory effect of the heterochromatin (Haruyama et al., 2009; Jones). Using multiple founder lines and screening can help to circumvent and control for these effects, but they require the use of more mice and resources. The transgenic mouse model remains a staple and indispensable research tool for developmental and cancer studies.

Mouse Mammary Tumor Virus and Organ Specific Mouse Models

The mouse mammary tumor virus, MMTV, also known as the Bittner virus, is an oncogenic RNA virus of the *retroviridae* family (Matsuzawa et al., 1995). The virus primarily targets and functions within the luminal alveolar cells and is transferred primarily from the milk of a mouse to another mouse. It initially infects the spleen before transitioning to the mammary gland (Matsuzawa et al., 1995). Within the mammary gland the virus causes tumorigenesis through insertional mutagenesis, a process by which it disrupts an already established genome, and induces subsequent activation of local oncogenes (JS et al., 2017; Taneja et al., 2009). One of the first genes identified to be activated by the MMTV was *Wnt1*; since this initial discovery up to 6 other oncogenes have also been identified (Cardiff and Kenney, 2011). The value in the discovery of the mouse mammary tumor virus is the use of its driving ability as a promoter (Taneja et al., 2009). Furthermore, MMTV is a mammary specific virus and therefore any gene constructs made using the MMTV promoter to drive up-regulation are most likely to be limited to the mammary, as well as other secretory organs such as kidneys, salivary glands, lungs and seminal vesicles (Muñoz and Bolander, 1989; Ross et al., 1990). The long terminal repeat of the MMTV promoter contains a hormone responsive element which is generally used in creating the myriad of provirus-integrated MMTV driven transgenic models. One such model was created in 1984 and placed the proto-oncogene C-Myc under the control of the MMTV promoter leading to the MMTV-Myc mouse (Stewart et al., 1984). This mouse developed mammary tumors after a year post-birth demonstrating the effects of elevated Myc expression. The MMTV promoter is activated post-birth due to its hormone-responsive element and its activity increases in pregnancy due to the

increase in systemic hormones such as prolactin, progesterone and other glucocorticoids (Ham et al., 1988). The MMTV promoter is an incredibly useful tool for manipulating genes within mouse models due to its specificity, constitutive activation and time-point activation.

Mammary Organoids, 3D culture and In-vitro models

Organoids are a relatively new and emerging technique. The idea of developing organoids began in the 1980s when culturing protocols began using 3D versus 2D culture and allowing cells to grow within various mediums (Ravi et al., 2015). Within the focus of mammary groups like Li et al. It was found that when culturing mouse primary cells on 2D culture they lost their ability to produce milk proteins even in the presence of lactogenic factors (Li et al., 1987). Subsequent studies determined that when culturing cells in a gel formed of Collagen I, the mRNA for milk proteins like β -casein increased (Li et al., 1987). With time, more complex organoid media containing Collagen I/IV, Fibronectin and other factors were generated that better mimicked the microenvironments of the modeled organs (Benton et al., 2009; Hughes et al., 2010). Gut organoids were some of the first to be established and gave a great deal of insight into the nature of the cell-cell adhesions and intricate signaling pathways necessary to differentiation (Date and Sato, 2015; Dutta et al., 2017). The ability of organoids to approximate the *in-vivo* environment of an organ system allows for the study of developmental mechanisms, differentiation states, and dynamics. This capacity of organoids also gives insight into cancer progression. Mammary organoids from both primary cells and cell lines are a useful model with several groups establishing their own (Jamieson et al., 2017; Zhang et al., 2017). This mammary organoid system and its establishment could be used as a high-throughput developmental system that could be easily manipulated with the factors added in media.

Hypothesis & Objectives

A known susceptibility window for cancer development and tumorigenesis during mammary development is puberty. Spy1 is a protein that has a variety of roles to play both in development and directly in driving the cell cycle and regulating proliferation.

We hypothesize that proper regulation of Spy1 is necessary for typical mammary development and elevated levels of Spy1 can lead to increased proliferation in ductal and lobalveolar development culminating in precocious mammary development. We further hypothesize that elevated Spy1 levels in a cell organoid system will increase proliferation and bud formation.

We aim to address this hypothesis through the following two objectives

- Characterize the effects on pubertal mammary branching, proliferation and finally the role of Spy1 in puberty using the MMTV-Spy1 mouse model.
- Dissect Spy1 effect on budding and branching using the Hc11 3D cell culture system.

This work will give new insight into the developmental effects and mechanistic effects of Spy1 using two different model system. This insight could be used to determine early indicator system of susceptibility using Spy1 levels and any morphological effects.

Materials and Methods

Mouse Maintenance

Mice were maintained following the Canadian Council on Animal Care Guidelines under the animal utilization protocol 17-17 approved by the University of Windsor. Mice (aged 10 and up) were sacrificed using a CO₂ gas chamber and tissues were then extracted following CCAC guidelines (Canadian Council on Animal Care, 2010).

Immunohistochemistry

Mouse inguinal glands were extracted and fixed overnight in 10% formalin at 4°C. The following day the tissues were dehydrated through a series of increasing ethanol washes (70%, 95%, 100%) for 2 hours in 70% ethanol and for 1 hour twice in 95% and left in 100% ethanol overnight. Tissues were then cleared in xylene for 1.5 hours and embedded in paraffin wax (Richard-Allan Scientific™ Histoplast Paraffin). Immunohistochemistry was performed as described in (Shore AN et al 2016 *Dev Biol.*). 5 µm sectioned slides were prepared from paraffin embedded mouse mammary glands using a microtome. Tissues were deparaffinized in xylene for 3 washes at 3 minutes each and rehydrated using descending ethanol concentrations (100%, 95%, 80% and 70%). Antigen retrieval was performed using 10mM sodium citrate buffer (pH=6) with 20-minute microwave heating. Endogenous peroxidases were quenched with 10% hydrogen peroxide solution. Blocking was done with Anti-rodent MOM blocker (Biocare Medical) or 2% Goat serum in 0.5% tween PBS solution for mouse and rabbit secondary antibodies respectively. Sections were incubated in primary antibodies, amphiregulin (Antibodies-Online No. ABIN704996) (1:600) and anti-BrdU (BD Biosciences No. 550891) (1:200) for 1 hour at 37°C and overnight at 4°C respectively. Biotinylated secondary antibodies were used at a concentration of 1:750 and were diluted in MOM blocker or 0.5% Tween in 1x PBS and applied for 45 minutes at room temperature. Slides were stained using ABC reagent kit (Vectastain ABC) and peroxidase activated 3,3'-diaminobenzidine substrate kit (Invitrogen) following manufacturer's instruction and left to stain for 10 minutes. Following DAB staining slides were left in water for 10 minutes. Hematoxylin was used as a nuclear counterstain and tissues were then dehydrated with a series of ethanol immersions (70%, 95%, 100%) and finally cleared in xylene overnight. The following day the tissues were mounted with permount

solution (Fisher Scientific SP15-100), imaged with Leica DMI6000 inverted microscope and analyzed with ImageJ colour deconvolution software.

Immunofluorescence

Inguinal glands were extracted and fixed as previously mentioned. 5 µm tissue sectioned slides were deparaffinized by two 30-minute washes in xylene. Tissues were then rehydrated using a descending series of ethanol washes (100%, 95%, 80%, 70%), all of which were performed for 15 minutes. Antigen retrieval was performed using a 10mM sodium citrate buffer solution (Ph=6) and microwaved (100°C) for 20 minutes. Following this, tissues were kept in Coplin glassware under running water for 15 minutes. Tissues were blocked with Anti-rodent MOM blocker (Biocare Medical) for 10 minutes. Sections were incubated with primary antibodies, anti-Spy1 (Abcam ab153965) (1:200) and anti-BrdU (BD Biosciences No. 550891) (1:200) overnight at 4°C and 1 hour at 37°C respectively. Sections were washed three times with 1x PBS for 5 minutes and blocked again between each application of primary antibody. Fluorescent secondary antibodies were used at concentrations of 1:250 (and were diluted in MOM blocker or 1% BSA with 1:250 DAPI (thermo) and applied for 15 minutes at room temperature. Slides were then washed 3 times with 1x PBS and mounted with anti-bleaching mounting medium (Vectashield). The following day tissues were imaged with Leica DMI6000 inverted microscope with Leica AF software.

Mammary Line Maintenance

Mouse mammary epithelial cells, HC11, (Provided by Dr. C Shemanko) were maintained in RPMI media (Hyclone) containing 10% New Born Calf Serum (vol/vol) (C8056; Sigma Aldrich), supplemented with 10ng/mL EGF (Life Technologies) ,5µg/mL bovine insulin (Sigma) and 0.5% Puromycin/Streptomycin (vol/vol). Cells were maintained at 5% CO₂ at 37°C.

Plasmids and Constructs

The pHIV Zsgreen vector or pEIZ (18121) was received as a gift from Bryan Welm & Zena Werb (Welm et al., 2008) while the pEIZ-Spy1 vector was generated as previously described (Lubanska et al., 2014)and was utilized in Spy1 overexpression experiments HC11 mammary cell lines.

Transfection

Transfection of HC11 mammary cell lines were performed as follows. Four hours prior to transfection and at 80% cell confluence, growth media was removed and replaced with serum and antibiotic free media. Cells were transfected using 25µg of polyethylenimine (PEI) and 12 µg of plasmid DNA. The DNA and PEI mix were incubated at room temp for 10 minutes before drop-wise addition to plate. Cells were then incubated for 18-24 hours before transfection media was removed.

Generating Mammary Organoids

Mammary organoids were generated using HC11 cells transfected with pEIZ and pEIZ-Spy1 vectors. Collagen gel was prepared using rat-tail collagen I (BD Bioscience #354326). We mixed 217uL of Collagen 1 with 25µl DMEMx10 and 8ul NaOH 1N and mixed lightly. Pre-assembled collagen solution was mixed until a pink colour was achieved, representing pH 7-7.5; pH was tested and adjusted accordingly otherwise. 25uL of the pre-assembled collagen solution was used to form a thin underlay on a 24-well plate. The plate was then incubated at 37 degrees until ready. The pre-assembled collagen solution was incubated in 4 degree for 2.5 hours. Collagen and Matrigel (Fisher Scientific Corning™ C356237; C354236 respectively) were mixed at a concentration of 7:3. 2000 cells were seeded in 50uL of collagen: Matrigel mix and plated onto the collagen underlay and incubated for 1 hour at 37 degrees. Specific media was then added to their respective wells (RPMI, RPMI+EGF, RPMI+FGF).

HC11 and Primary Cell Organoid Analysis

HC11 cell organoids were considered mature upon reaching a size of >30 µm in diameter due to their clear visibility (Nguyen-Ngoc et al., 2015). Mature organoids were then sorted into either budding/stratified or non-budding groups and counted separately. In each media condition (RPMIS, RPMI +EGF, RPMI +FGF), the budding/stratified organoids were divided by total counted per image with four images randomly taken per time-point. All counting was done in ImageJ with images exported into the software and counted.

Primary cell organoids were allowed to grow for two weeks before imaging and subsequent paraffin embedding. Size was measured in primary cell organoids using ImageJ by determining the length and width of each organoids per image and calculating the area in µm². The branches were counted per primary organoid and averages reported over three measurements.

Quantitative Real Time PCR Analysis

RNA was isolated using Qiagen RNeasy extraction kit as per manufactures instructions (Qiagen, Cat.74106). Quality and concentration of RNA was analyzed with Nanodrop lite Spectrophotometer (Thermofisher). Subsequent cDNA was made using Quanta qScript (II) as per manufacturer's instructions. Real time PCR was optimized for use of SyberGreen (Applied Biosystems) and analyzed using Vii7 Real Time PCR system (Life Technology) and associated software. The primers used were as follows:

Flag-Tagged Spy1 Forward 5' TGACAAGAGGCACAATCAGATGT 3'

Flag-Tagged Spy1 Reverse 5' CAAATAGGACGCTTCAGAGTAATGG 3'

Mouse GAPDH Forward 5' GATGCCCCATGTTTGTGAT 3'

Mouse GAPDH Reverse 5' GTGGTCATGAGCCCTCCA 3'

Whole Mount Production and Analysis

Extracted inguinal glands were placed on a positively charged glass slide (Thomas Scientific) and left in Clarke's solution (75% ethanol 25% acetic acid) overnight. Following this, the tissues were placed in 70% ethanol for 30 minutes and moved into carmine solution (0.2% carmine alum and 0.5% potassium sulphate) until red stain was visible throughout the gland. Glands were then de-stained in a 1% HCl 70% Ethanol solution for 6 hours and dehydrated in increasing ethanol concentrations (70%,95%,100%) for 15 minutes respectively. Tissues were cleared in xylene overnight and mounted with Permount solution (Fisher Scientific SP15-100). Slides were imaged using Leica MZFLIII dissecting microscope (Leica Microsystems) and data was captured using Leica LASv4.3 Software (Leica Application Suite).

Mammary Epithelial Content Analysis

Mammary epithelial content analysis was done by exporting whole mount images of all timepoints into ImageJ and then setting the image to 8-bit and grayscale. An image containing a line measuring 1mm is used to set the mm to pixel conversion rate under the analysis tabs so that the final measurement in ImageJ is equivalent to millimeters. Following this, the image tab is selected, and the threshold tab is brought up. The threshold value is increased until the black image covers the developing glands and tissues but not the entire whole-mount. This value is

measured as the area of epithelial tissue. The threshold is then selected again and increased until the entire whole-mount is covered. This value is measured and represents the total whole-mount size. The percentage of epithelial tissue per whole-mount is acquired by dividing the first value by the second.

Mammary Lateral Branch Analysis

Mammary lateral branch analysis was done by exporting time-point specific whole mount images into ImageJ and setting the pixel conversion scale to the equivalent distance of the 50 um scalebar in the image. Any measurements taken of the length using ImageJ were then converted to millimeters. Five ducts were selected per image with the length and number of branches measured.

BrdU Incorporation Assay

The 8-week-old MMTV-Spy1 mouse and its control littermates received an intraperitoneal injection of 50 mg/kg of Bromodeoxyuridine (BD Pharmingen). 2 hours post injection the mouse was sacrificed, and tissue was collected for histology. Once stained positive cells which expressed brown colour in the nucleus were counted as positive and divided by the total number of blue hematoxylin stained cells per gland.

Image Analysis and Quantification

ImageJ was used to quantify differences in protein densitometry from tissues stained with immunohistochemistry. Once images were opened in imageJ software colour deconvolution was selected and applied to H-dab setting with integrated density selected as the output. Only the brown (DAB) and blue (Hematoxylin) channels were used; once a channel was selected the image was limited to the threshold. Each image was then automatically adjusted to its threshold and the value recorded. The values of the brown channel were divided by the blue control hematoxylin channel to normalize each measurement. The normalized values were averaged to determine the densitometry.

Statistical Analysis

Graphpad Prism 5.0 software was utilized for statistical analysis. Data is presented as differences between the means and standard error. Two-way ANOVA was used for analysis of lateral branching and total epithelial content in MMTV-Spy1 mice and control with Bonferroni's post-hoc

test to further elucidate time-point specific differences. Uneven n-values were normalized through weighted means detailed in LD Fisher and G vanBelle (Brunner, 1998). Two-way ANOVA with repeated measures was used for analysis of differences between organoid media conditions with repeated measures and Bonferroni's post-hoc within media condition. Students T-test was used where applicable, such as analysis of immunofluorescence imaging in BrdU injected mice and analysis of primary cell organoids, (* $p < 0.05$) was considered as significant in all cases.

Results

Spy1 upregulation causes increased lateral side branching and mammary density

Puberty is a developmental timepoint during which there is a known associated risk of breast cancer as compared to other early life events (Bodicoat et al., 2014). A key feature of development during puberty is expansion of the ductal network. Previous work has shown that MMTV-Spy1 mice have significant increase in the total number of lateral branches at 6 weeks of age (Fifield, 2015). Therefore, to assess the extent of Spy1 effects on lateral branching, we extracted inguinal glands from MMTV-Spy1 and control littermates at 6, 8 and 12 weeks of age and whole mount analysis was performed. Lateral branching was analyzed by assessing the number of lateral branching points along the primary ducts. There was an overall effect of Spy1 up-regulation seen between MMTV-Spy1 mice and their littermate controls. Specifically, at 6 weeks we saw a significant 52% ($p < 0.05$) increase in the number of lateral branches per mm of the primary duct. This same result was seen in both 8 and 12-week glands with a 55% and 38% ($p < 0.005$) increase respectively (Figure 3A, B). Since there was an increase in lateral branching, we then investigated whether this lead to an increase in epithelial content within the fat pad, which is a known marker for tumorigenesis along with increased mammary density (Huo et al., 2015). We evaluated the total epithelial cell content and found an overall increase in epithelial content in the MMTV-Spy1 mice as compared to the littermate controls. However, we did not find a significant difference at any one specific time-point (Figure 3C).

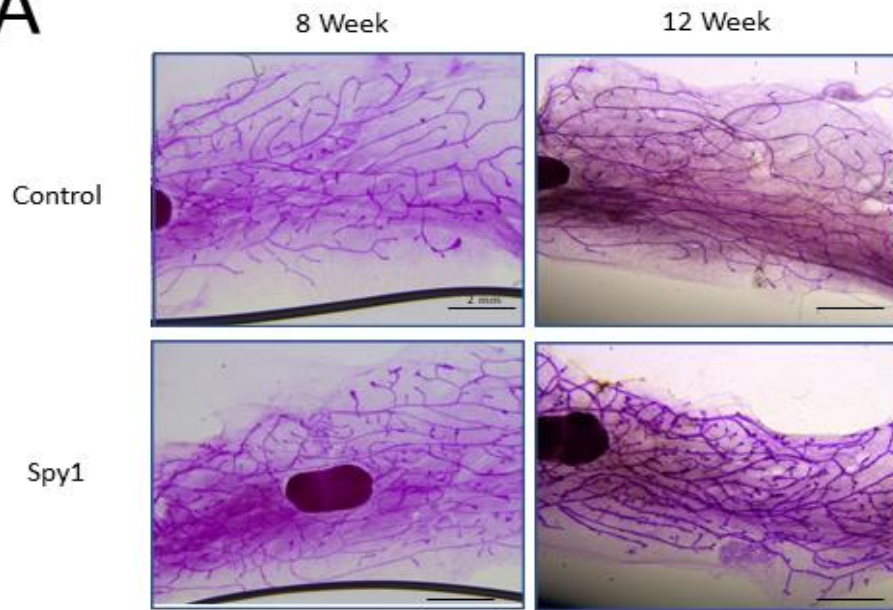
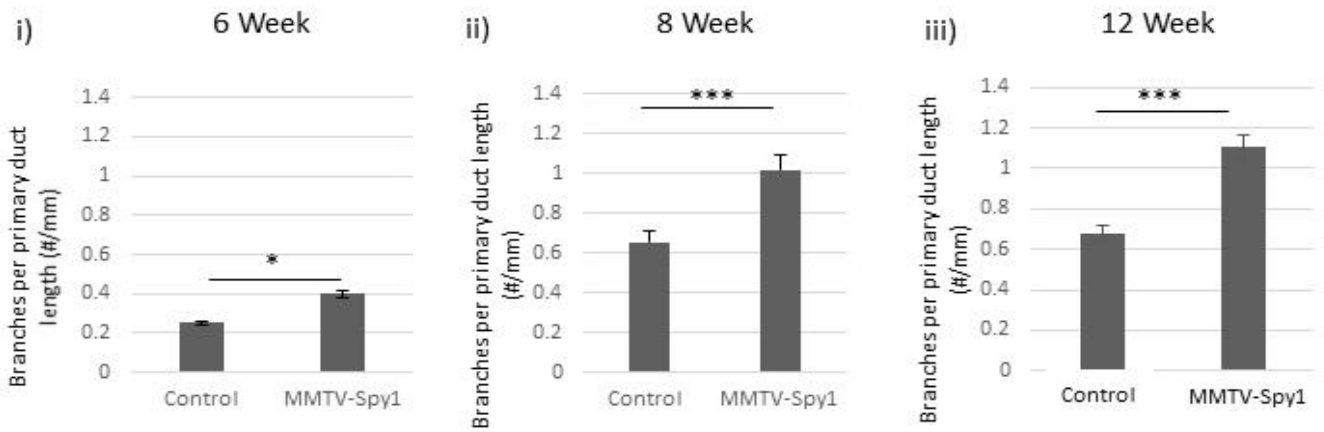
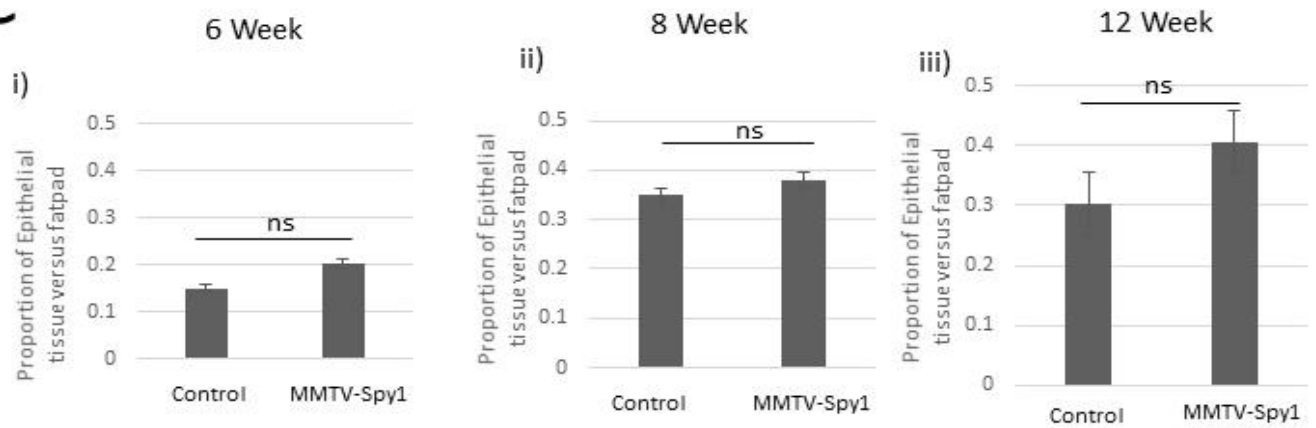
A**B****C**

Figure 3: Whole Mount analysis of Control versus MMTV-Spy1 glands during puberty. A) Representative images of carmine stained whole mounts from, 8 weeks and 12-week FVB mice (6-week n=4, 8-week n=4, 12-week n=3). B) Analysis of wholemount images from control and MMTV-Spy1 inguinal glands. Number of branches off the primary duct were counted and then divided by the length of each primary duct to determine the proportion of branches/mm for i) 6 week ii) 8 week and iii) 12-week glands. C) Analysis of total epithelial content in area of ducts divided by total area of fat pad with Bonferroni post-hoc showing differences at individual time-points i) 6 weeks ii) 8 weeks iii) 12 weeks. (* = $p < 0.05$) Error bars represent standard error SEM.

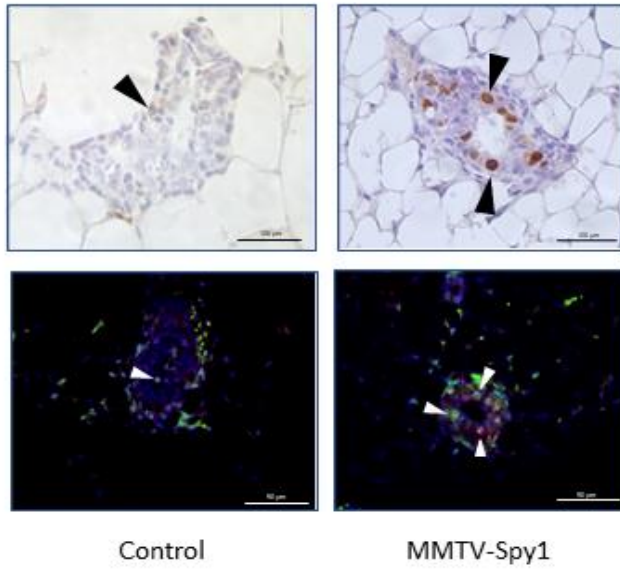
Spy1 increases mammary epithelial proliferation and secretion of AREG in the pubertal and adult mammary gland

Since Spy1 is known to increase proliferation (Porter et al., 2002), the increase in side branching may be due to enhanced proliferation. To investigate whether or not Spy1 is enhancing proliferation we intraperitoneally injected 8-week MMTV-Spy1 mice and their control littermates with BrdU. After tissue extraction and IHC for anti-BrdU we found that the MMTV-Spy1 mice had a significant increase in BrdU positive cells ($p < 0.05$) over their littermate controls (Figure 4A, B, Supplementary Figure 1A, B). Immunofluorescence co-staining for BrdU and Spy1 in developing 8-week glands revealed a higher proportion of nuclei in MMTV-Spy1 glands co-staining for BrdU and Spy1 than their control counterparts (Figure 4.C, D). This data demonstrates that MMTV-Spy1 mice have increased rates of proliferation, and Spy1 significantly correlates with BrdU expression in these mice.

We previously described the EGFR pathway involving the AREG agonist that is actively used in mammary development, specifically in lateral branching and growth involving the ductal epithelial cells. Previous work has shown that Spy1 can activate the estrogen receptor without the need of its hormone ligand, therefore we wanted to investigate the role of Spy1 on this pathway to determine if this may be contributing to the significant increase in proliferation seen. The developing ducts of 6-week, 8-week and 12-week mice were analyzed for AREG expression via immunohistochemistry and we found a main effect of Spy1 up-regulation as an overall higher level of AREG in the MMTV-Spy1 glands versus their littermate controls. Specifically, there was a significantly higher level of AREG at 12 weeks and a non-significant difference at 6-week. We observed no difference in AREG in 8-week MMTV-Spy1 glands (Figure 4B, C). This data demonstrates that Spy1 enhances proliferation and this may be due in part to alterations in EGF and AREG signaling.

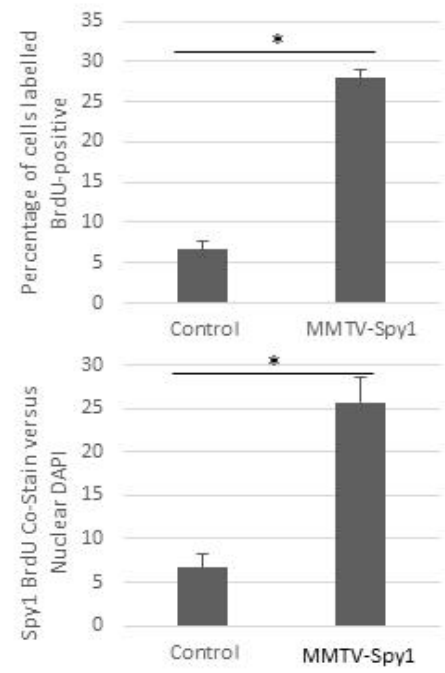
A

8 Week

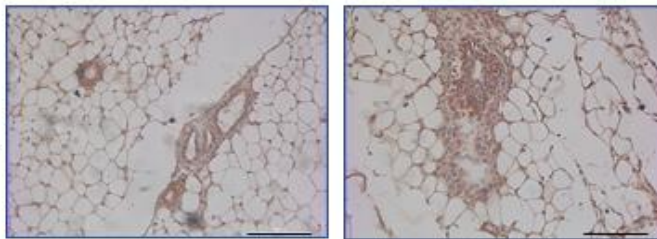


Control

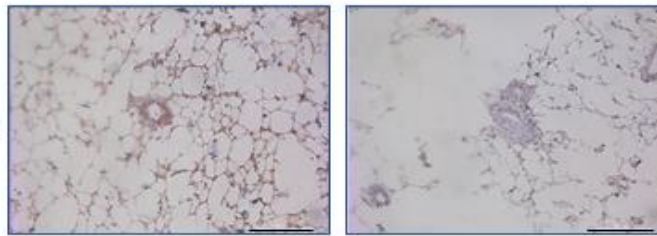
MMTV-Spy1

B**C**

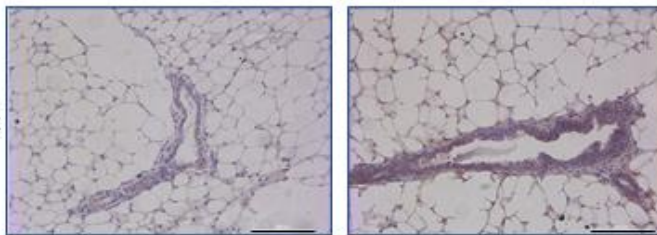
6 Week



8 Week



12 Week



Control

MMTV-Spy1

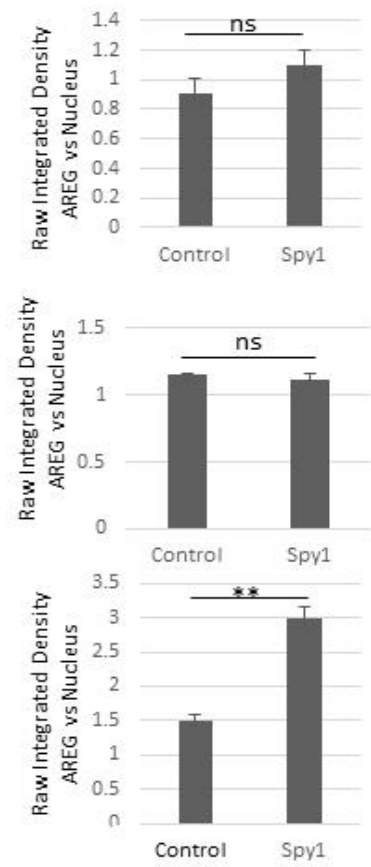
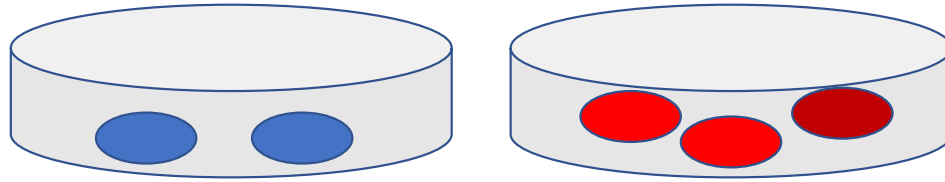
D

Figure 4 MMTV-Spy1 mammary glands have higher proliferation and AREG levels: A) Representative images of BrdU IHC staining in 8-week control and MMTV-Spy1 glands (Black and white arrows represent positive BrdU and Brdu/Spy1 stained cells respectively). Scale bars represent 100 μ m and 50 μ m respectively. B) Graphical representations of percentage of stained nuclei divided by total nuclei in gland of 8-week control and MMTV-Spy1(n=3). C) Representative images of AREG IHC in control and MMTV-Spy1 glands at 6, 8 and 12 weeks respectively (6-week n=4, 8-week n=3, 12-week n=3) Scale bars represent 100 μ m. D) Graphical representations of total AREG staining normalized to hematoxylin. Raw densitometry values integrated using ImageJ. (* = p <0.05, ** = p<0.01). Error bars represent SEM.

Spy1 increases budding capacity in mammary epithelial cells

3D culture is a useful technique due to its ability to better replicate *in vivo* environments but offer the ability to focus on specific aspects of those environments. Therefore, we turned our attention to *in vitro* 3D to determine the ability of Spy1 to initiate lateral branching and proliferation by narrowing the focus to its mechanistic ability to affect budding and growth using the mammary epithelial cell line, HC11 (Figure 5). We overexpressed Spy1 in HC11 cells using a pEIZ-Spy1 vector, while our control HC11s were transfected with an empty pEIZ vector (Figure 5). pEIZ is a bacterial DNA plasmid with insertion sites that allows for the production of specific proteins when present inside mammalian cells (Welm et al., 2008). We then grew HC11-Spy1 and HC11 control cells in 3D Matrigel-Collagen culture with Base RPMI media supplemented with either serum (Figure 6. A i)), serum and EGF (Figure 6.A ii) or serum and FGF (Figure 6.A iii)). EGF and FGF were chosen as additives due to both having the ability to induce proliferation with FGF2 being a known branching factor and EGFs shown to induce branching in certain conditions (Chen et al., 2012; Clevers, 2016). We then imaged the 3D culture cells every 24 hours for a week (Figure 5. B). We investigated the number of organoids that were budding as opposed to simply forming spheres and reported the percentage of budding organoids to total counter organoids per group (Figure 5). There was a main effect of Spy1 up-regulation on both the base serum (RPMIS) and EGF supplemented media (EGF) but not in FGF supplemented media (FGF). At 24 hours only EGF organoids showed a difference in budding between pEIZ and pEIZ-Spy1 (Figure 6.A, C). Similarly, at 48 hours only the EGF organoids show a difference between pEIZ and pEIZ-Spy1 with the Spy1 organoids budding at significantly higher percentages (Figure 5 C). At 72 the differences between the organoids have caught up with no significant difference between all three media conditions (Figure 6 .C). Interestingly, there was no overall effect of Spy1 overexpression on FGF media (Figure 6.C). The data demonstrates that Spy1 significantly enhances the budding of mammary epithelial cells in both the presence and absence of growth factors.



pEIZ

pEIZ-Spy1



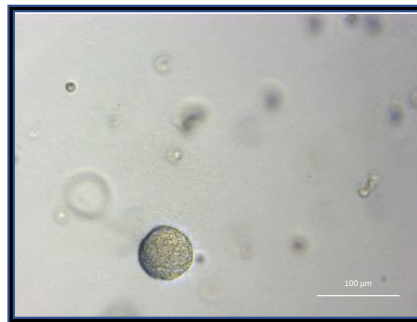
Culture in 3:7 Matrigel
Collagen I Mix



RPMIS

RPMI
+EGF

RPMIS
+FGF



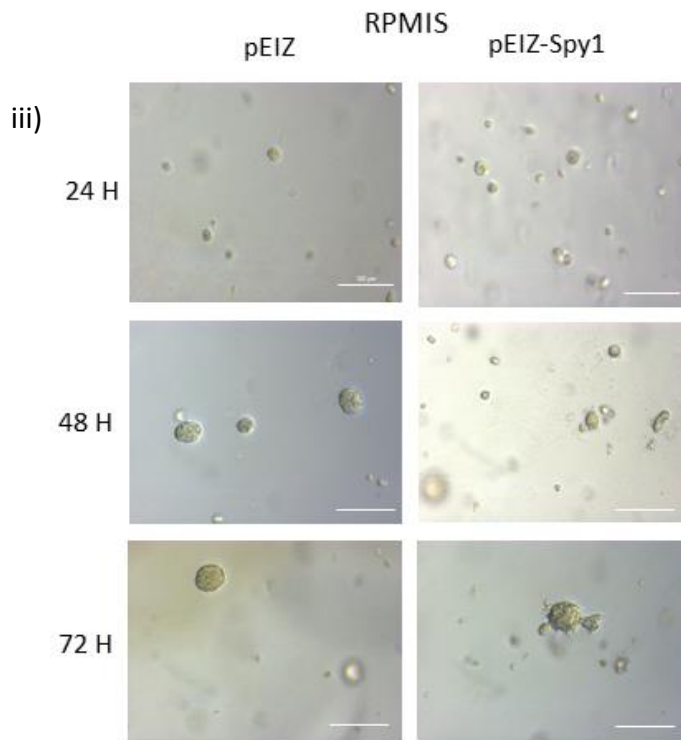
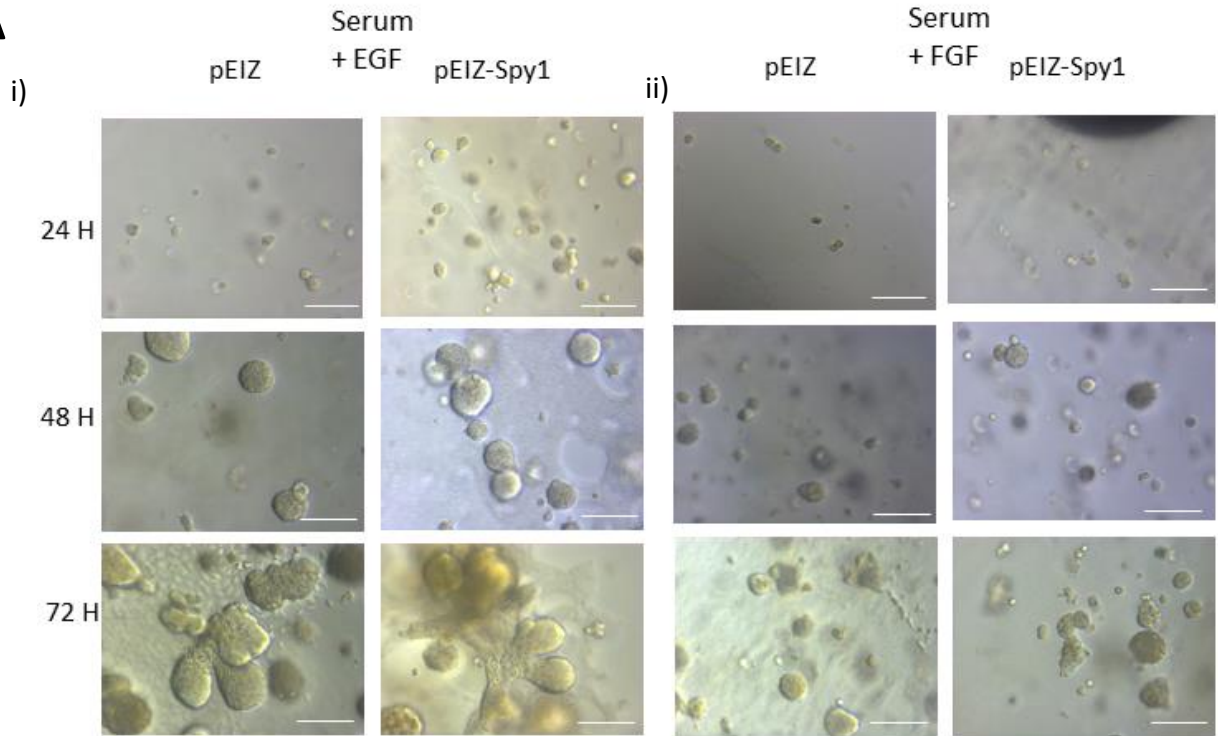
Non-budding Spheroid



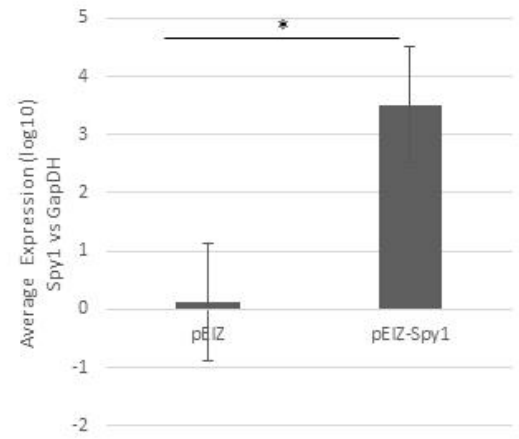
Budding Organoid

Figure 5: **Schematic of organoid preparation and production.** pEIZ and pEIZ-Spy1 HC11 cells were cultured in 3:7 Matrigel Collagen mix with 3 different media conditions. RPMIS represents base RPMI media with serum and insulin. RPMI + EGF represents RPMI media with serum and insulin as well as EGF supplemented. RPMI + FGF represents RPMI media supplemented with serum, insulin and FGF. The final images represent budding versus non-budding organoids.

A



B



C

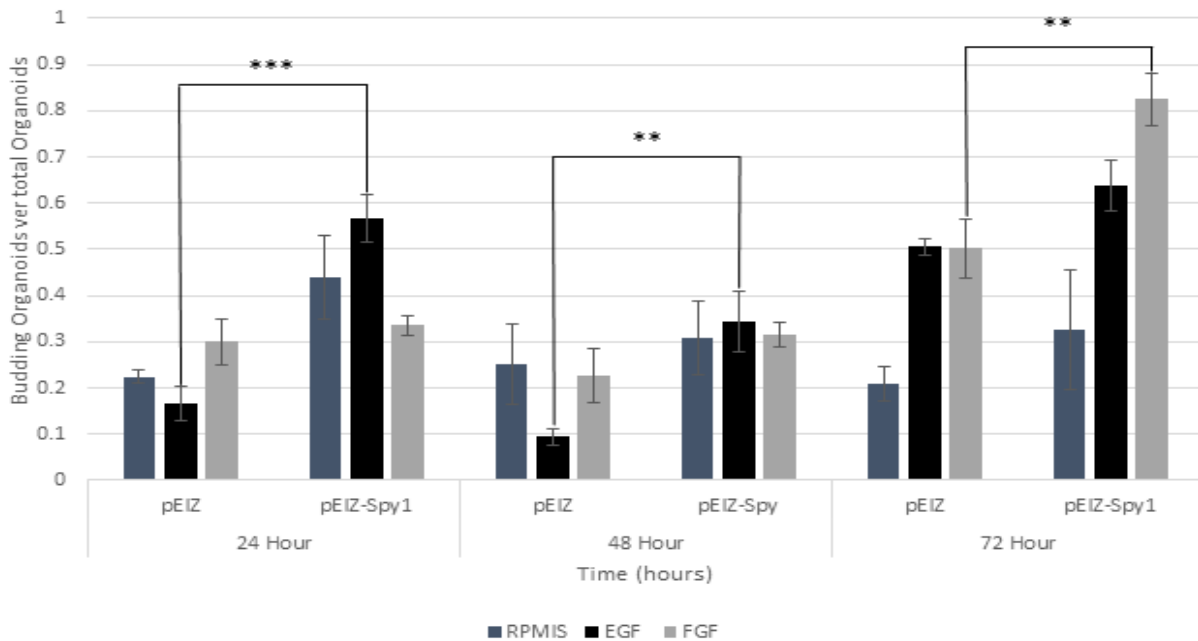
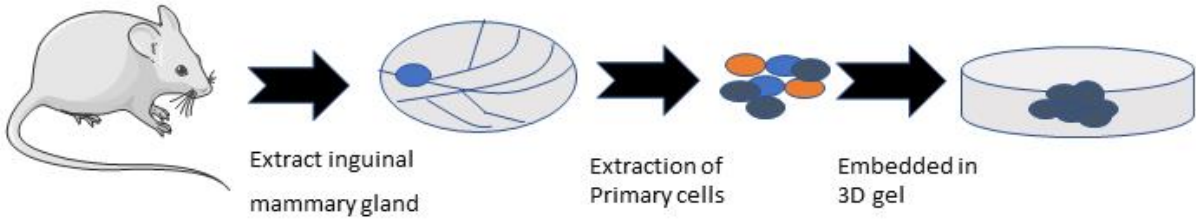


Figure 6: **Spy1 up-regulated HC11 Organoids have higher rates of budding.** A) Representative images of organoids taken at 24h, 48h and 72h timepoints. Each image represents organoids grown in either i) serum and EGF ii) serum and FGF iii) serum alone B) qRT-PCR analysis of HC11 cells transfected with pEIZ and pEIZ-Spy1 for Spy1 levels and corrected for GAPDH (n=3). C) Graphical representation of the proportion of budding organoids divided by the total number of organoids at 3 timepoints (* = $p < 0.05$, ** = $p < 0.01$, *** = $p < 0.001$). Error bars represent SEM.

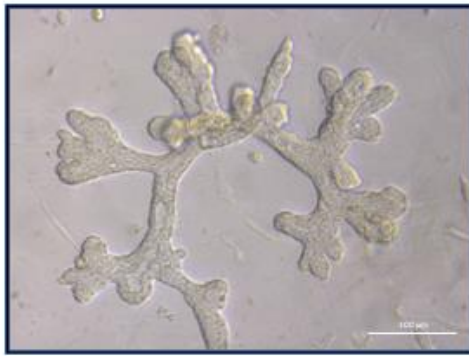
MMTV-Spy1 mouse primary cell organoids have higher budding capacity

To verify the results seen using Spy1 overexpressing HC11 cells, primary mammary epithelial cells were extracted from 8-week-old MMTV-Spy1 mice and their littermate controls and cultured in 3D Matrigel-Collagen. Organoids were allowed to grow for two weeks and total size and budding capacity per organoid was evaluated (Figure 7A, B). We found that the MMTV-Spy1 primary cell organoids at plating density of 2500 cells had significantly more buds formed per organoid than their counterpart controls, while there was a non-significant difference in their sizes (Figure 7C i)). At a plating density of 1000 cells, the MMTV-Spy1 organoids were significantly larger with no difference in the budding capacity (Figure 7C ii)). These results led us to conclude that the MMTV-Spy1 primary organoids had more growth at low density and quicker budding cues at higher cell densities.

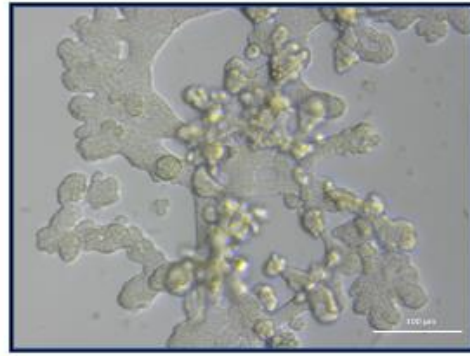
A



B



Control



MMTV-Spy1

C

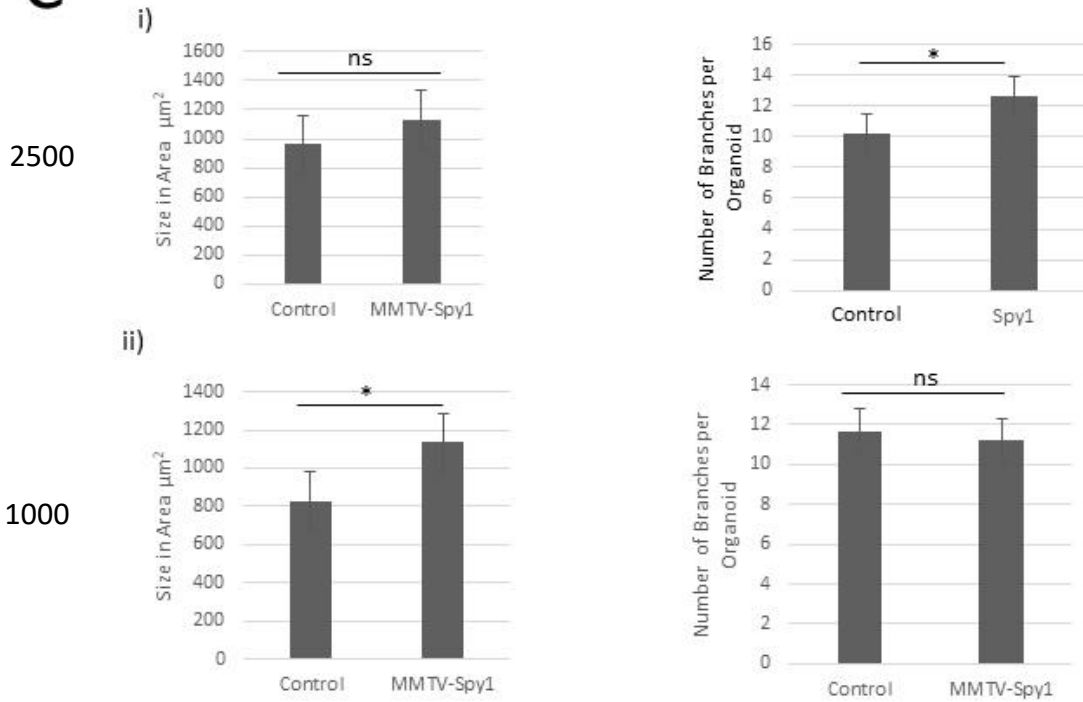
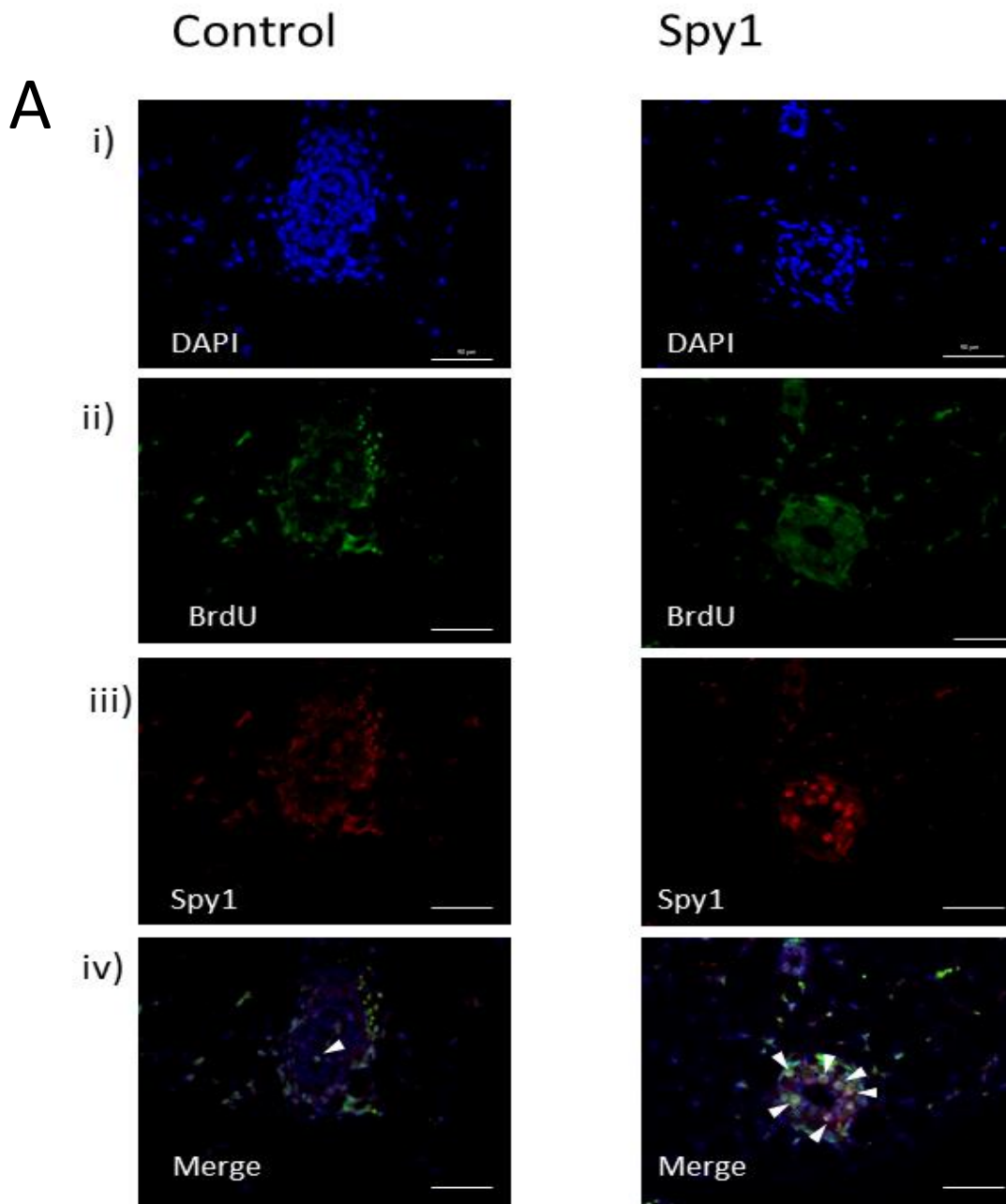


Figure 7 MMTV-Spy1 primary cell organoids have more growth and branching *in vitro*: A) Schematic for extraction of primary cells from mice and growth in Matrigel-Collagen Media. B) Representative images of MMTV-Spy1 primary cell extracted organoids and control cell organoids. C) i) Representative images of 2500 density grown cells comparing size and number of branches per organoid ii) Representative images of 1000 density grown cells comparing size and number of branches per organoid. (* = $p < 0.05$). Error bars represent SEM



Supplementary Figure 1 **Extended immunofluorescence channels for Spy1 and BrdU**: A) BrdU and Spy1 Co-stain IF with channel splits and higher resolution i) DAPI ii) GFP channel iii) Spy1 TXR channel iv) Merge

Discussion

Increases in lateral branching during mammary development can be a sign of both proliferation and mis-regulation of the known branching phenotypes (Weber et al., 2017). Either mis-regulation or hyper-proliferation can be meaningful stepping stones to tumorigenesis and can increase susceptibility to cancer (Weber et al., 2017). Investigation into lateral branching phenotypes are typically done to note either decrease in proliferation or precocious growth. The phenotype in Figure 3.A showed a significant increase lateral branching. However, unlike other precocious branching phenotypes we did not witness an increase in ductal elongation (Li et al., 2002). This contrast suggests that Spy1 is having a specific effect on the mechanisms governing lateral side branching but not ductal elongation, such as levels of FGF2. Similarly, the increased total epithelial content seen in Figure 3.B is a known susceptibility marker for tumorigenesis and breast cancer in humans (Martin and Boyd, 2008). These phenotypes support the idea that Spy1 exerts direct effects on mammary lateral branching through increased proliferation.

When the initial budding to form a lateral side branch has occurred, any number of growth factors can continue the elongation of the branch (Nelson et al., 2006). The EGFR pathway that contributes to proliferation in lateral branching and within the ductal epithelium has a number of possible agonists: EGF-1, AREG and TGF- α (Aupperlee et al., 2013; Brisken and O'Malley, 2010; Sternlicht and Sunnarborg, 2008). In Figure 4.B we show an overall difference in AREG levels between MMTV-Spy1 glands and the counterpart control. A significant effect of time was observed as well likely due to the effects of Spy1 being more prominent as size and proliferative capacity of the gland grew. Specifically, we saw a significant difference at 12-weeks and a meaningful but non-significant difference at 6-weeks. However, we saw no difference in AREG levels at 8-weeks likely due the previous time-point having already begun the process of proliferation and the regulation of AREG therefore being cyclic (McBryan et al., 2008). A way to investigate this would be to check AREG levels, using immunohistochemistry, at 4-weeks and 16-18 weeks to get a better profile of its abundance in the developing gland.

This increase in AREG in the MMTV-Spy1 mice may possibly contribute to the growth of the ductal buds leading to the phenotype seen in Figure 3. While this data shows us the plausible effects of Spy1 on two major mammary pathways further investigation into those pathways would be necessary. The aforementioned stromal epithelial EGFR pathway has many downstream targets

from the EGFR receptor, including its own activation, whose abundance and activation levels could give insight to the full effects of Spy1 on this pathway and subsequently how Spy1 causes the increased proliferation we see in Figure 4.A. Furthermore, staining for AREG using immunohistochemistry while useful does not differentiate between secreted and surface level AREG. If the phenotypic effect seen is not due to total increased abundance of AREG but rather higher level of AREG cleaved from the membrane and secreted into the stromal epithelial cleft, then the increase in temporal AREG would be due to increased activation of ADAM17 g-coupled protein and Spy1 would therefore have an effect on enzymatic activation rather than driving increased expression of AREG (McBryan et al., 2008; Sternlicht and Sunnarborg, 2008). Investigating mRNA levels of AREG and comparing them to IHC and protein levels of total abundance would determine if more AREG is produced or more is cleaved. Spy1 could also be affecting the TGF- β inhibitory pathway known to control the location and abundance of lateral branching. The TGF- β inhibitory pathways downstream targets activate the Cip/Kip family p27 and p21 both of which are known to arrest the cell cycle and halt proliferation when activated. In literature Spy1 has been shown to cause the degradation of p27 through E3 mediated poly-ubiquitination and has been also shown to be less affected by p21 inhibition (Al Sorkhy et al., 2016). It is therefore possible that Spy1 up-regulation in the gland is acting downstream of TGF- β and negating the inhibitory aspects of the consistently activated pathway, leading to more initiation budding events. Modulation of TGF- β signaling could lead to increased lateral branching through decreased activation of Wnt5A and subsequent non-canonical *Wnt* signaling. Therefore, investigating phosphorylation status of Ror2 receptor in the mammary epithelium would determine if canonical *Wnt* activation is a component of Spy1 up-regulation. Additionally, decreased SLIT activation could also increase the number of myoepithelial cells which has been shown to increase the amount of lateral branching (Macias et al., 2011). However, no measured change in the myoepithelium was seen.

The formation of organoids/3D culture from cell lines in Engelbreth-Holm-Swarm (EHS) mouse sarcoma secreted Matrigel is a useful assay for determining growth, stemness and self-organizing capacity (Jamieson et al., 2017; Nguyen-Ngoc et al., 2015; Ravi et al., 2015). The ability of cells to self-organize and form structures reminiscent of their *in vivo* counterpart organs is one of the many ways that the organoid assay can give insights into the cues and pathways at work in development. Using HC11 cells transfected with pEIZ-Spy1 and pEIZ we investigated the ability of 3D cultures to form spheres and eventually budding/branching structures that mimic the

architecture of the developing mammary gland. We were primarily interested in their ability to form buds under minimal (serum alone RPMIS), normal (serum + EGF), and enhanced (serum + FGF) conditions and what this could tell us about the cues Spy1 is affecting *in vitro* (Figure 4).

We found that Spy1 in both the minimal and normal conditions had an overall main effect (Figure 6.C) and showed significant differences at two timepoints (24 hours ,48 hour). Significant differences between pEIZ and pEIZ Spy1 in EGF supplemented media were seen at 24 and 48 hours but not at 72 hours (Figure 6.C i) ii)). Increased directional budding in pEIZ-Spy1 organoids in higher proportion than simple sphere formation suggests some of the aforementioned mechanisms. Furthermore, the increased budding proportion in the pEIZ-Spy1 organoids has similarities to the *in-vivo* branching phenotype seen in the mice. If Spy1 up-regulation only increased proliferation, then in the early timepoints (24 hours) the proportion of budding organoids to total would likely be lower in the Spy1 upregulated HC11 cells than their counterpart controls as more simple sphere organoids would form but would not bud at a higher rate than control. Therefore, this would lower the proportion of budding in the pEIZ-Spy1 organoids. The early timepoints in the serum + FGF media condition organoids show no significant difference in the proportion of budding organoids to total between pEIZ-Spy1 and pEIZ HC11 cells (Figure 6.C iii)). While there is a significant effect of time on the growing organoids suggesting that in the presence of FGF2 the effects of Spy1-upregulation are silenced. This could be due to the immediate effects of Spy1 mediated through down-stream targets of the FGFR pathway (Ornitz and Itoh, 2015). This data demonstrates that Spy1 can enhance budding. Furthermore, this data when paired with the previous organoids conditions suggests that Spy1 plays an important role in budding/branching.

While this assay was insightful, its scope suffered limitations. Firstly, size could not be measured properly between organoids as eventual outgrowth blurs the ability to image and maintaining track of the same organoids. Secondly, with extended time measurements it was difficult to keep track of cell death in the organoid media so any extended timing for organoid growth in-advisable due lack of discrimination. Embedding of organoids into agarose/paraffin and sectioning for Immunofluorescence would be a logical and necessary next step in determining if the TGF- β and EGFR pathways are indeed affected by Spy1 up-regulation. Furthermore, investigating polarity effects on the mammary architecture is a logical next step as cell polarity and asymmetry are necessary components of a complex organ system (Ochoa-Espinosa and Affolter, 2012). Staining

for golgin subfamily member A2 (Gm-130) and cytokeratin 18 (CK18) and 14 (CK14) would be logical next steps in determining apical cell polarity and epithelial luminal concentration.

To study the effects of Spy1 on budding in primary cells we proceeded to extract mammary cells from MMTV-Spy1- and littermate controls and grow them in Matrigel/Collagen medium according to the schematic in Figure 7.A. These primary cells were plated at cell densities of 1000 and 2500 and allowed to grow for two weeks before imaging. We then randomly imaged several 3D organoids per mouse. We evaluated the organoids for total area in μm^2 and number of branches per organoid. We found that at a plating density of 1000 cell per 10cm plate the MMTV-Spy1 organoids were significantly larger than their littermate controls but did not have more branches per organoid (Figure 7.B i). However, at the 2500 cell plating density we found that the opposite trend was true, wherein the MMTV-Spy1 organoids had significantly more branches per organoid than their littermate controls but were no longer significantly larger (Figure 7.B ii). The growth differences associated with plating densities may indicate Spy1's ability to increase proliferation leading to the formation of larger organoids at a faster rate. It is possible that the effects of Spy1 in organoid budding require a specific size before leading to branch initiation events. In the 2500 cell plating both the organoids have caught up in their size and have begun cues for branching and cell rearrangement; at this point Spy1 could be working through the TGF- β pathway to increase the number of budding events and through EGFR to continue elongation.

This data highlights the ability of Spy1 to increase mammary budding, mammary epithelial cell density and proliferation *in-vivo* and increase budding and size *in-vitro*. Disruption of mammary architecture and increased proliferation and branching are all stepping stones to tumorigenesis and mimic mechanisms used by aggressive cancers to grow and invade (McBryan et al., 2008; Moses and Barcellos-Hoff, 2011). When investigating Spy1 levels in tissue and tumor databases the human protein atlas has it not to be present in normal tissues in high abundance. While may play a role in establishment of the primary tumor after initiation and subsequent expansion; the HPA does not show high abundance of Spy1 in breast cancer (Thul et al., 2017; Uhlen et al., 2017; Uhlén et al., 2015)(data available from <https://www.proteinatlas.org/ENSG00000163806-SPDYA/tissue/breast>. Conversely, in work done by Al Sorkhy et al and others has shown spy1 to be elevated several aggressive human cancers, including breast and liver that often use developmental pathways to advance and invade (Al Sorkhy et al., 2012; Jin et al., 2018; Ke et al., 2009).Furthermore, Golipour et al has demonstrated spy1 being maintained at high abundance

during post-pubertal mammary development. While the results here do not directly connect to the data seen in breast cancer studies, they do provide correlative evidence which may link these phenotypes to cancer development. An important step in linking the results in this work to known cancer pathways would be to determine if indeed Spy1 and other oncogenic genes are affecting developmental pathways examined here, in different types of breast cancer.

Future Experiments

Future experiments could include a more thorough dissection of the AREG and TGF- β pathways using qRT, WB and IHC so that the full effect of Spy1 up-regulation could be seen. This would therefore determine which pathways are most involved in the phenotypes and which could be potential targets for therapy. In the mouse model, continuing the investigation to include earlier time-points such as 4 weeks would give insight into the rise of AREG levels in mouse mammary development as well as the initiation of proliferation both in the control mouse and in the MMTV-Spy1 mouse. While differences between levels of AREG have been visualized at 12 weeks the absence of a significant difference at 6 and 8 weeks, suggests other pathways involved in proliferation or a staggered effect of AREG. Similarly, collecting mice at 7 weeks would increase the range of analysis and determine when AREG levels in the control mice catch up to the MMTV-Spy1. While MMTV-Spy1 mice have higher levels of proliferation and BrdU/Spy1 co-staining at 8 weeks, determining levels of proliferation at the 6- and 12-week time-points would give a more thorough understanding of the phenotype. Our work demonstrates Spy1 can increase proliferation in mammary development and regulated AREG levels further corroborating the work done by Golipour et al (Golipour et al., 2008).

When bound to EGF-1 the EGFR receptor is abrogated after activation while binding to AREG does not elicit this reaction (Kappler et al., 2015; Kerpedjieva et al., 2012). Therefore, continued investigation into the levels of other EGFR ligands, such as EGF-1 and TGF- α , is required to determine the effects of Spy1 on mammary developmental pathways that include EGFR. Furthermore, AREG and EGF-1 have differing downstream targets while they both signal through EGFR (Macdonald-Obermann and Pike, 2014). Investigation into the levels of these downstream targets would better elucidate the full effect of these pathways and determine new possible targets for cancer therapy. Willmarth et al has shown AREG to be a novel target for breast cancer therapy and with further investigation from our work more targets could be determined (Willmarth and Ethier, 2008).

In this work we also investigated HC11 organoid budding under three specific media conditions (see Figure 5). The HC11 3D culture could be treated with TGF- β agonists or activators for its downstream targets, p21, p27 and Ror2 to determine if the pEIZ-Spy1 phenotype can be reduced back to its control counterpart. Organoids could also be developed with serum-free media conditions and different EGFR ligands introduced, such as AREG, EGF-1, TGF- α , to determine which are more impactful in organoid budding and growth rates. Conversely, Spy1 knockout organoids could be developed with similar media conditions to explore the possible consequences of Spy1 loss on budding and growth. Preliminary data from other groups in our lab developing a Crispr/Cas9 Spy1 knockout cell line show a lack of Spy1 causes differentiation in HC11 cell lines. Therefore, investigating if these cell lines could form organoids under serum-free and growth enriched media conditions would give further insight into Spy1's role as a mitogen.

While not shown in this work, paraffin embedding and hematoxylin-eosin staining of the organoids was successful. Using this technique organoids collected from the multiple media conditions could be embedded, sectioned and evaluated using immunohistochemistry and fluorescence. This data demonstrates Spy1's ability to manipulate developmental pathways, such as EGFR, in a similar manner to cancer (Moses and Barcellos-Hoff, 2011). Therefore, Spy1 levels could be used as a potential marker of susceptibility to tumorigenesis and possibly breast cancer.

REFERENCES/BIBLIOGRAPHY

- Al Sorkhy, M., Ferraiuolo, R.-M., Jalili, E., Malysa, A., Fratiloiu, A.R., Sloane, B.F., and Porter, L.A. (2012). The cyclin-like protein Spy1/RINGO promotes mammary transformation and is elevated in human breast cancer. *BMC Cancer* *12*, 45.
- Al Sorkhy, M., Fifield, B.-A., Myers, D., and Porter, L.A. (2016). Direct interactions with both p27 and Cdk2 regulate Spy1-mediated proliferation in vivo and in vitro. *Cell Cycle* *15*, 128–136.
- Anderson, S.M., Rudolph, M.C., McManaman, J.L., and Neville, M.C. (2007). Secretory activation in the mammary gland: it's not just about milk protein synthesis! *J. Mammary Gland Biol. Neoplasia* *9*, 14.
- Aupperlee, M.D., Leipprandt, J.R., Bennett, J.M., Schwartz, R.C., and Haslam, S.Z. (2013). Amphiregulin mediates progesterone-induced mammary ductal development during puberty. *Breast Cancer Res.* *15*.
- Ball, R.K., Friis, R.R., Schoenenberger, C.A., Doppler, W., and Groner, B. (1988). Prolactin regulation of beta-casein gene expression and of a cytosolic 120-kd protein in a cloned mouse mammary epithelial cell line. *EMBO J.* *7*, 2089–2095.
- Barnes, E.A., Porter, L.A., Lenormand, J.-L., Dellinger, R.W., and Donoghue, D.J. (2003). Human Spy1 Promotes Survival of Mammalian Cells following DNA Damage. *Cancer Res.* *63*, 3701–3707.
- Barnum, K.J., and O'Connell, M.J. (2014). Cell Cycle Regulation by Checkpoints. *Methods Mol. Biol.* Clifton NJ *1170*, 29–40.
- Bellusci, S., Grindley, J., Emoto, H., Itoh, N., and Hogan, B.L. (1997). Fibroblast growth factor 10 (FGF10) and branching morphogenesis in the embryonic mouse lung. *Dev. Camb. Engl.* *124*, 4867–4878.
- Benton, G., George, J., Kleinman, H.K., and Arnaoutova, I.P. (2009). Advancing science and technology via 3D culture on basement membrane matrix. *J. Cell. Physiol.* *221*, 18–25.
- Besson, A., Dowdy, S.F., and Roberts, J.M. (2008). CDK Inhibitors: Cell Cycle Regulators and Beyond. *Dev. Cell* *14*, 159–169.
- Biro, F.M., and Deardorff, J. (2013). Identifying Opportunities for Cancer Prevention During Preadolescence and Adolescence: Puberty as a Window of Susceptibility. *J. Adolesc. Health* *52*, S15–S20.
- Bodicoat, D.H., Schoemaker, M.J., Jones, M.E., McFadden, E., Griffin, J., Ashworth, A., and Swerdlow, A.J. (2014). Timing of pubertal stages and breast cancer risk: the Breakthrough Generations Study. *Breast Cancer Res. BCR* *16*, R18.
- Borel, F., Lacroix, F.B., and Margolis, R.L. (2002). Prolonged arrest of mammalian cells at the G1/S boundary results in permanent S phase stasis. *J. Cell Sci.* *115*, 2829–2838.
- Brennan, K.R., and Brown, A.M.C. (2004). Wnt Proteins in Mammary Development and Cancer. *J. Mammary Gland Biol. Neoplasia* *9*, 119–131.

- Brisken, C., and O'Malley, B. (2010). Hormone action in the mammary gland. *Cold Spring Harb. Perspect. Biol.* 2, a003178.
- Brunner, E. (1998). *Biostatistics. A Methodology for the Health Sciences.* L. D. Fisher and G. van Belle, Wiley, New York, 1993. No. of pages: xxii+991. Price: £37.50 (Paperback). ISBN 0-4711-6609-X. *Stat. Med.* 17, 2805–2806.
- Cai, C., Yu, Q.C., Jiang, W., Liu, W., Song, W., Yu, H., Zhang, L., Yang, Y., and Zeng, Y.A. (2014). R-spondin1 is a novel hormone mediator for mammary stem cell self-renewal. *Genes Dev.* 28, 2205–2218.
- Canadian Council on Animal Care (2010). *CCAC guidelines on: euthanasia of animals used in science.* (Ottawa: Canadian Council on Animal Care).
- Cánepa, E.T., Scassa, M.E., Ceruti, J.M., Marazita, M.C., Carcagno, A.L., Sirkin, P.F., and Ogara, M.F. (2007). INK4 proteins, a family of mammalian CDK inhibitors with novel biological functions. *IUBMB Life* 59, 419–426.
- Cao, X.R., Lill, N.L., Boase, N., Shi, P.P., Croucher, D.R., Shan, H., Qu, J., Sweezer, E.M., Place, T., Kirby, P.A., et al. (2008). Nedd4 Controls Animal Growth by Regulating IGF-1 Signaling. *Sci. Signal.* 1, ra5.
- Cardiff, R.D., and Kenney, N. (2011). A compendium of the mouse mammary tumor biologist: from the initial observations in the house mouse to the development of genetically engineered mice. *Cold Spring Harb. Perspect. Biol.* 3.
- Cardiff, R.D., and Wellings, S.R. (1999). The Comparative Pathology of Human and Mouse Mammary Glands. *J. Mammary Gland Biol. Neoplasia* 4, 105–122.
- Chapman, R.S., Lourenco, P., Tonner, E., Flint, D., Selbert, S., Takeda, K., Akira, S., Clarke, A.R., and Watson, C.J. (2000). The role of Stat3 in apoptosis and mammary gland involution. Conditional deletion of Stat3. *Adv. Exp. Med. Biol.* 480, 129–138.
- Chen, C.-L., Yu, X., James, I.O.-A., Zhang, H., Yang, J., Radulescu, A., Zhou, Y., and Besner, G.E. (2012). Heparin-binding EGF-like Growth Factor Protects Intestinal Stem Cells from Injury in a Rat Model of Necrotizing Enterocolitis. *Lab. Investig. J. Tech. Methods Pathol.* 92, 331–344.
- Cheng, A., Xiong, W., Ferrell, J.E., and Solomon, M.J. (2005a). Identification and comparative analysis of multiple mammalian Speedy/Ringo proteins. *Cell Cycle Georget. Tex* 4, 155–165.
- Cheng, A., Gerry, S., Kaldis, P., and Solomon, M.J. (2005b). Biochemical characterization of Cdk2-Speedy/Ringo A2. *BMC Biochem.* 6, 19.
- C.H.Streuli, S.P. (1996). Requirement of basement membrane for the suppression of programmed cell death in mammary epithelium | *Journal of Cell Science.*
- Clevers, H. (2016). Modeling Development and Disease with Organoids. *Cell* 165, 1586–1597.

- Cowin, P., and Wysolmerski, J. (2010). Molecular mechanisms guiding embryonic mammary gland development. *Cold Spring Harb. Perspect. Biol.* *2*, a003251.
- Date, S., and Sato, T. (2015). Mini-gut organoids: reconstitution of the stem cell niche. *Annu. Rev. Cell Dev. Biol.* *31*, 269–289.
- Denicourt, C., and Dowdy, S.F. (2004). Cip/Kip proteins: more than just CDKs inhibitors. *Genes Dev.* *18*, 851–855.
- Dinarina, A., Perez, L.H., Davila, A., Schwab, M., Hunt, T., and Nebreda, A.R. (2005). Characterization of a new family of cyclin-dependent kinase activators. *Biochem. J.* *386*, 349–355.
- Dinarina, A., Santamaria, P.G., and Nebreda, A.R. (2009). Cell cycle regulation of the mammalian CDK activator RINGO/Speedy A. *FEBS Lett.* *583*, 2772–2778.
- Dontu, G., and Ince, T.A. (2015). Of Mice and Women: A Comparative Tissue Biology Perspective of Breast Stem Cells and Differentiation. *J. Mammary Gland Biol. Neoplasia* *20*, 51–62.
- Doyle, A., McGarry, M.P., Lee, N.A., and Lee, J.J. (2012). The Construction of Transgenic and Gene Knockout/Knockin Mouse Models of Human Disease. *Transgenic Res.* *21*, 327–349.
- Dutta, D., Heo, I., and Clevers, H. (2017). Disease Modeling in Stem Cell-Derived 3D Organoid Systems. *Trends Mol. Med.* *23*, 393–410.
- Ercan, C., van Diest, P.J., and Vooijs, M. (2011). Mammary development and breast cancer: the role of stem cells. *Curr. Mol. Med.* *11*, 270–285.
- Ferby, I., Blazquez, M., Palmer, A., Eritja, R., and Nebreda, A.R. (1999). A novel p34cdc2-binding and activating protein that is necessary and sufficient to trigger G2/M progression in *Xenopus* oocytes. *Genes Dev.* *13*, 2177–2189.
- Ferraiuolo, R.-M., Tubman, J., Sinha, I., Hamm, C., Porter, L.A., Ferraiuolo, R.-M., Tubman, J., Sinha, I., Hamm, C., and Ann Porter, L. (2017). The cyclin-like protein, SPY1, regulates the ER α and ERK1/2 pathways promoting tamoxifen resistance. *Oncotarget* *8*, 23337–23352.
- Fifield, B.-A. (2015). Generation of Model Systems for the Study of Novel Cell Cycle Regulation in Development: Implications for Spy1 in Tumour Susceptibility. *Electron. Theses Diss.*
- Flanders, K.C., and Wakefield, L.M. (2009). Transforming growth factor- β s and mammary gland involution; functional roles and implications for cancer progression. *J. Mammary Gland Biol. Neoplasia* *14*, 131.
- Flores, J.M., Martín-Caballero, J., and García-Fernández, R.A. (2014). p21 and p27 a shared senescence history. *Cell Cycle* *13*, 1655–1656.
- Forrester, E., Chytil, A., Bierie, B., Aakre, M., Gorska, A.E., Sharif-Afshar, A.-R., Muller, W.J., and Moses, H.L. (2005). Effect of Conditional Knockout of the Type II TGF- β Receptor Gene in

Mammary Epithelia on Mammary Gland Development and Polyomavirus Middle T Antigen Induced Tumor Formation and Metastasis. *Cancer Res* 8.

Golipour, A., Myers, D., Seagroves, T., Murphy, D., Evan, G.I., Donoghue, D.J., Moorehead, R.A., and Porter, L.A. (2008). The Spy1/RINGO Family Represents a Novel Mechanism Regulating Mammary Growth and Tumorigenesis. *Cancer Res.* 68, 3591–3600.

Gordon, J.W., Scangos, G.A., Plotkin, D.J., Barbosa, J.A., and Ruddle, F.H. (1980). Genetic transformation of mouse embryos by microinjection of purified DNA. *Proc. Natl. Acad. Sci. U. S. A.* 77, 7380–7384.

Green, K.A., and Lund, L.R. (2005). ECM degrading proteases and tissue remodelling in the mammary gland. *BioEssays News Rev. Mol. Cell. Dev. Biol.* 27, 894–903.

Ham, J., Thomson, A., Needham, M., Webb, P., and Parker, M. (1988). Characterization of response elements for androgens, glucocorticoids and progestins in mouse mammary tumour virus. *Nucleic Acids Res.* 16, 5263–5276.

Hanahan, D., Wagner, E.F., and Palmiter, R.D. (2007). The origins of oncomice: a history of the first transgenic mice genetically engineered to develop cancer. *Genes Dev.* 21, 2258–2270.

Hannezo, E., Scheele, C.L.G.J., Moad, M., Drogo, N., Heer, R., Sampogna, R.V., Rheenens, J. van, and Simons, B.D. (2017). A Unifying Theory of Branching Morphogenesis. *Cell* 171, 242-255.e27.

Harashima, H., Dissmeyer, N., and Schnittger, A. (2013). Cell cycle control across the eukaryotic kingdom. *Trends Cell Biol.* 23, 345–356.

Haruyama, N., Cho, A., and Kulkarni, A.B. (2009). Overview: engineering transgenic constructs and mice. *Curr. Protoc. Cell Biol. Chapter 19*, Unit 19.10.

Hens, J.R., and Wysolmerski, J.J. (2005). Key stages of mammary gland development: Molecular mechanisms involved in the formation of the embryonic mammary gland. *Breast Cancer Res.* 7.

Hilska, M., Collan, Y.U., O Laine, V.J., Kössi, J., Hirsimäki, P., Laato, M., and Roberts, P.J. (2005). The significance of tumor markers for proliferation and apoptosis in predicting survival in colorectal cancer. *Dis. Colon Rectum* 48, 2197–2208.

Hinck, L., and Silberstein, G.B. (2005). Key stages in mammary gland development: The mammary end bud as a motile organ. *Breast Cancer Res.* 7.

Hughes, K., and Watson, C.J. (2012). The spectrum of STAT functions in mammary gland development. *JAK-STAT* 1, 151–158.

Hughes, C.S., Postovit, L.M., and Lajoie, G.A. (2010). Matrigel: A complex protein mixture required for optimal growth of cell culture. *PROTEOMICS* 10, 1886–1890.

Huo, C.W., Chew, G., Hill, P., Huang, D., Ingman, W., Hodson, L., Brown, K.A., Magenau, A., Allam, A.H., McGhee, E., et al. (2015). High mammographic density is associated with an

- increase in stromal collagen and immune cells within the mammary epithelium. *Breast Cancer Res.* *17*, 79.
- Iber, D., and Menshykau, D. (2013). The control of branching morphogenesis. *Open Biol.* *3*, 130088.
- Ikink, G.J., Boer, M., Bakker, E.R.M., Vendel-Zwaagstra, A., Klijn, C., Ten Hove, J., Jonkers, J., Wessels, L.F., and Hilken, J. (2018). Insertional mutagenesis in a HER2-positive breast cancer model reveals ERAS as a driver of cancer and therapy resistance. *Oncogene* *37*, 1594–1609.
- Inman, J.L., Robertson, C., Mott, J.D., and Bissell, M.J. (2015). Mammary gland development: cell fate specification, stem cells and the microenvironment. *Development* *142*, 1028–1042.
- Jackson, P.K. (2008). The Hunt for Cyclin. *Cell* *134*, 199–202.
- Jamieson, P.R., Dekkers, J.F., Rios, A.C., Fu, N.Y., Lindeman, G.J., and Visvader, J.E. (2017). Derivation of a robust mouse mammary organoid system for studying tissue dynamics. *Development* *144*, 1065–1071.
- Jin, Q., Liu, G., Bao, L., Ma, Y., Qi, H., Yun, Z., Dai, Y., and Zhang, S. (2018). High Spy1 expression predicts poor prognosis in colorectal cancer. *Cancer Manag. Res.* *10*, 2757–2765.
- Johnson, R.H., Chien, F.L., and Bleyer, A. (2013). Incidence of Breast Cancer With Distant Involvement Among Women in the United States, 1976 to 2009. *JAMA* *309*, 800–805.
- Jones, D. (2011). Genetic Engineering of a Mouse. *Yale J. Biol. Med.* *84*, 117–124.
- Jones, D. Genetic Engineering of a Mouse. *8*.
- JS, L., CC, N., WK, G., and DD, T. (2017). Mouse mammary tumour virus (MMTV) and human breast cancer with neuroendocrine differentiation. *Infect. Agent. Cancer* *12*.
- Kappler, C.S., Guest, S.T., Irish, J.C., Garrett-Mayer, E., Kratche, Z., Wilson, R.C., and Ethier, S.P. (2015). Oncogenic signaling in amphiregulin and EGFR-expressing PTEN-null human breast cancer. *Mol. Oncol.* *9*, 527–543.
- Karaiskou, A., Perez, L.H., Ferby, I., Ozon, R., Jesus, C., and Nebreda, A.R. (2001). Differential Regulation of Cdc2 and Cdk2 by RINGO and Cyclins. *J. Biol. Chem.* *276*, 36028–36034.
- Ke, Q., Ji, J., Cheng, C., Zhang, Y., Lu, M., Wang, Y., Zhang, L., Li, P., Cui, X., Chen, L., et al. (2009). Expression and prognostic role of Spy1 as a novel cell cycle protein in hepatocellular carcinoma. *Exp. Mol. Pathol.* *87*, 167–172.
- Kerpedjieva, S.S., Kim, D.S., Barbeau, D.J., and Tamama, K. (2012). EGFR Ligands Drive Multipotential Stromal Cells to Produce Multiple Growth Factors and Cytokines via Early Growth Response-1. *Stem Cells Dev.* *21*, 2541–2551.
- Lenormand, J.L., Dellinger, R.W., Knudsen, K.E., Subramani, S., and Donoghue, D.J. (1999). Speedy: a novel cell cycle regulator of the G2/M transition. *EMBO J.* *18*, 1869–1877.

- Li, G., Robinson, G.W., Lesche, R., Martinez-Diaz, H., Jiang, Z., Rozengurt, N., Wagner, K.-U., Wu, D.-C., Lane, T.F., Liu, X., et al. (2002). Conditional loss of PTEN leads to precocious development and neoplasia in the mammary gland. *Dev. Camb. Engl.* *129*, 4159–4170.
- Li, M., Liu, X., Robinson, G., Bar-Peled, U., Wagner, K.U., Young, W.S., Hennighausen, L., and Furth, P.A. (1997). Mammary-derived signals activate programmed cell death during the first stage of mammary gland involution. *Proc. Natl. Acad. Sci. U. S. A.* *94*, 3425–3430.
- Li, M.L., Aggeler, J., Farson, D.A., Hatier, C., Hassell, J., and Bissell, M.J. (1987). Influence of a reconstituted basement membrane and its components on casein gene expression and secretion in mouse mammary epithelial cells. *Proc. Natl. Acad. Sci. U. S. A.* *84*, 136–140.
- Lim, S., and Kaldis, P. (2013). Cdks, cyclins and CKIs: roles beyond cell cycle regulation. *Development* *140*, 3079–3093.
- Lin, Y., Zhang, S., Rehn, M., Itäranta, P., Tuukkanen, J., Heljäsvaara, R., Peltoketo, H., Pihlajaniemi, T., and Vainio, S. (2001). Induced repatterning of type XVIII collagen expression in ureter bud from kidney to lung type: association with sonic hedgehog and ectopic surfactant protein C. *Dev. Camb. Engl.* *128*, 1573–1585.
- Liu, C. (2013). Strategies for Designing Transgenic DNA Constructs. *Methods Mol. Biol.* Clifton NJ *1027*.
- Lubanska, D., Market-Velker, B.A., deCarvalho, A.C., Mikkelsen, T., Fidalgo da Silva, E., and Porter, L.A. (2014). The Cyclin-like Protein Spy1 Regulates Growth and Division Characteristics of the CD133+ Population in Human Glioma. *Cancer Cell* *25*, 64–76.
- Lund, L.R., Rømer, J., Thomasset, N., Solberg, H., Pyke, C., Bissell, M.J., Danø, K., and Werb, Z. (1996). Two distinct phases of apoptosis in mammary gland involution: proteinase-independent and -dependent pathways. *Dev. Camb. Engl.* *122*, 181–193.
- Macdonald-Obermann, J.L., and Pike, L.J. (2014). Different Epidermal Growth Factor (EGF) Receptor Ligands Show Distinct Kinetics and Biased or Partial Agonism for Homodimer and Heterodimer Formation. *J. Biol. Chem.* *289*, 26178–26188.
- Macias, H., Moran, A., Samara, Y., Moreno, M., Compton, J.E., Harburg, G., Strickland, P., and Hinck, L. (2011). SLIT/ROBO1 signaling suppresses mammary branching morphogenesis by limiting basal cell number. *Dev. Cell* *20*, 827–840.
- Makarenkova, H.P., Hoffman, M.P., Beenken, A., Eliseenkova, A.V., Meech, R., Tsau, C., Patel, V.N., Lang, R.A., and Mohammadi, M. (2009). Differential Interactions of FGFs with Heparan Sulfate Control Gradient Formation and Branching Morphogenesis. *Sci. Signal.* *2*, ra55.
- Malumbres, M. (2014). Cyclin-dependent kinases. *Genome Biol.* *15*, 122.
- Malumbres, M., and Barbacid, M. (2009). Cell cycle, CDKs and cancer: a changing paradigm. *Nat. Rev. Cancer* *9*, 153–166.

- Marlow, R., Strickland, P., Lee, J.S., Wu, X., PeBenito, M., Binnewies, M., Le, E.K., Moran, A., Macias, H., Cardiff, R.D., et al. (2008). SLITs Suppress Tumor Growth In vivo by Silencing Sdf1/Cxcr4 within Breast Epithelium. *Cancer Res.* *68*, 7819–7827.
- Marti, A., Feng, Z., Altermatt, H.J., and Jaggi, R. (1997). Milk accumulation triggers apoptosis of mammary epithelial cells. *Eur. J. Cell Biol.* *73*, 158–165.
- Martin, L.J., and Boyd, N.F. (2008). Mammographic density. Potential mechanisms of breast cancer risk associated with mammographic density: hypotheses based on epidemiological evidence. *Breast Cancer Res. BCR* *10*, 201.
- Martinez, A.M., Afshar, M., Martin, F., Cavadore, J.C., Labbé, J.C., and Dorée, M. (1997). Dual phosphorylation of the T-loop in cdk7: its role in controlling cyclin H binding and CAK activity. *EMBO J.* *16*, 343–354.
- Matsuzawa, A., Nakano, H., Yoshimoto, T., and Sayama, K. (1995). Biology of mouse mammary tumor virus (MMTV). *Cancer Lett.* *90*, 3–11.
- McAndrew, C.W., Gastwirt, R.F., and Donoghue, D.J. (2009). The atypical CDK activator Spy1 regulates the intrinsic DNA damage response and is dependent upon p53 to inhibit apoptosis. *Cell Cycle Georget. Tex* *8*, 66–75.
- McBryan, J., Howlin, J., Napoletano, S., and Martin, F. (2008). Amphiregulin: Role in Mammary Gland Development and Breast Cancer. *J. Mammary Gland Biol. Neoplasia* *13*, 159–169.
- McGrath, D.A., Fifield, B.-A., Marceau, A.H., Tripathi, S., Porter, L.A., and Rubin, S.M. (2017). Structural basis of divergent cyclin-dependent kinase activation by Spy1/RINGO proteins. *EMBO J.* *36*, 2251–2262.
- Moser, A.R., Hegge, L.F., and Cardiff, R.D. Genetic Background Affects Susceptibility to Mammary Hyperplasias and Carcinomas in ApcMin/± Mice. *7*.
- Moses, H., and Barcellos-Hoff, M.H. (2011). TGF- Biology in Mammary Development and Breast Cancer. *Cold Spring Harb. Perspect. Biol.* *3*, a003277–a003277.
- Mulac-Jericevic, B., Lydon, J.P., DeMayo, F.J., and Conneely, O.M. (2003). Defective mammary gland morphogenesis in mice lacking the progesterone receptor B isoform. *Proc. Natl. Acad. Sci.* *100*, 9744–9749.
- Muñoz, B., and Bolander, F.F. (1989). Prolactin regulation of mouse mammary tumor virus (MMTV) expression in normal mouse mammary epithelium. *Mol. Cell. Endocrinol.* *62*, 23–29.
- Nakayama, K., and Nakayama, K. (1998). Cip/Kip cyclin-dependent kinase inhibitors: brakes of the cell cycle engine during development. *BioEssays News Rev. Mol. Cell. Dev. Biol.* *20*, 1020–1029.
- Nakayama, K., Ishida, N., Shirane, M., Inomata, A., Inoue, T., Shishido, N., Horii, I., Loh, D.Y., and Nakayama, K. (1996). Mice lacking p27(Kip1) display increased body size, multiple organ hyperplasia, retinal dysplasia, and pituitary tumors. *Cell* *85*, 707–720.

Narod, S.A., and Salmena, L. (2011). BRCA1 and BRCA2 mutations and breast cancer. *Discov. Med.* *12*, 445–453.

Nebreda, A.R., and Hunt, T. (1993). The c-mos proto-oncogene protein kinase turns on and maintains the activity of MAP kinase, but not MPF, in cell-free extracts of *Xenopus* oocytes and eggs. *EMBO J.* *12*, 1979–1986.

Nelson, W.J. (2009). Remodeling Epithelial Cell Organization: Transitions Between Front–Rear and Apical–Basal Polarity. *Cold Spring Harb. Perspect. Biol.* *1*.

Nelson, C.M., VanDuijn, M.M., Inman, J.L., Fletcher, D.A., and Bissell, M.J. (2006). Tissue Geometry Determines Sites of Mammary Branching Morphogenesis in Organotypic Cultures. *Science* *314*, 298–300.

Nguyen-Ngoc, K.-V., Shamir, E.R., Huebner, R.J., Beck, J.N., Cheung, K.J., and Ewald, A.J. (2015). 3D Culture Assays of Murine Mammary Branching Morphogenesis and Epithelial Invasion. In *Tissue Morphogenesis*, C.M. Nelson, ed. (New York, NY: Springer New York), pp. 135–162.

Noble, M.E.M., and Endicott, J.A. (2001). Cyclin-Dependent Kinases. In *Encyclopedia of Genetics*, S. Brenner, and J.H. Miller, eds. (New York: Academic Press), pp. 500–506.

Nwabo Kamdje, A.H., Takam Kamga, P., Tagne Simo, R., Vecchio, L., Seke Etet, P.F., Muller, J.M., Bassi, G., Lukong, E., Kumar Goel, R., Mbo Amvene, J., et al. (2017). Developmental pathways associated with cancer metastasis: Notch, Wnt, and Hedgehog. *Cancer Biol. Med.* *14*, 109–120.

Oakes, S.R., Hilton, H.N., and Ormandy, C.J. (2006). Key stages in mammary gland development - The alveolar switch: coordinating the proliferative cues and cell fate decisions that drive the formation of lobuloalveoli from ductal epithelium. *Breast Cancer Res.* *8*, 207.

O’Brien, J., Martinson, H., Durand-Rougely, C., and Schedin, P. (2012). Macrophages are crucial for epithelial cell death and adipocyte repopulation during mammary gland involution. *Dev. Camb. Engl.* *139*, 269–275.

Ochoa-Espinosa, A., and Affolter, M. (2012). Branching Morphogenesis: From Cells to Organs and Back. *Cold Spring Harb. Perspect. Biol.* *4*.

Oftedal, O.T. (2002). The Mammary Gland and Its Origin During Synapsid Evolution. *J. Mammary Gland Biol. Neoplasia* *7*, 225–252.

Olsson, H., Baldetorp, B., Fernö, M., and Perfekt, R. (2003). Relation between the rate of tumour cell proliferation and latency time in radiation associated breast cancer. *BMC Cancer* *3*, 11.

Ornitz, D.M., and Itoh, N. (2015). The Fibroblast Growth Factor signaling pathway. *Wiley Interdiscip. Rev. Dev. Biol.* *4*, 215–266.

Parmar, H., and Cunha, G.R. (2004). Epithelial–stromal interactions in the mouse and human mammary gland in vivo. *Endocr. Relat. Cancer* *11*, 437–458.

- Parvani, J.G., Taylor, M.A., and Schiemann, W.P. (2011). Noncanonical TGF- β Signaling During Mammary Tumorigenesis. *J. Mammary Gland Biol. Neoplasia* 16, 127–146.
- Porter, L.A., and Donoghue, D.J. (2003). Cyclin B1 and CDK1: nuclear localization and upstream regulators. *Prog. Cell Cycle Res.* 5, 335–347.
- Porter, L.A., Dellinger, R.W., Tynan, J.A., Barnes, E.A., Kong, M., Lenormand, J.-L., and Donoghue, D.J. (2002). Human Speedy: a novel cell cycle regulator that enhances proliferation through activation of Cdk2. *J. Cell Biol.* 157, 357–366.
- Prasad, A., Paruchuri, V., Preet, A., Latif, F., and Ganju, R.K. (2008). Slit-2 Induces a Tumor-suppressive Effect by Regulating β -Catenin in Breast Cancer Cells. *J. Biol. Chem.* 283, 26624–26633.
- Quereda, V., Porlan, E., Cañamero, M., Dubus, P., and Malumbres, M. (2016). An essential role for Ink4 and Cip/Kip cell-cycle inhibitors in preventing replicative stress. *Cell Death Differ.* 23, 430–441.
- Rajaram, R.D., Buric, D., Caikovski, M., Ayyanan, A., Rougemont, J., Shan, J., Vainio, S.J., Yalcin-Ozuysal, O., and Briskin, C. (2015). Progesterone and Wnt4 control mammary stem cells via myoepithelial crosstalk. *EMBO J.* 34, 641–652.
- Ravi, M., Paramesh, V., Kaviya, S.R., Anuradha, E., and Solomon, F.D.P. (2015). 3D cell culture systems: advantages and applications. *J. Cell. Physiol.* 230, 16–26.
- Richert, M.M., Schwertfeger, K.L., Ryder, J.W., and Anderson, S.M. (2000). An atlas of mouse mammary gland development. *J. Mammary Gland Biol. Neoplasia* 5, 227–241.
- Roarty, K., and Serra, R. (2007). Wnt5a is required for proper mammary gland development and TGF- β -mediated inhibition of ductal growth. *Development* 134, 3929–3939.
- Roarty, K., Shore, A.N., Creighton, C.J., and Rosen, J.M. (2015). Ror2 regulates branching, differentiation, and actin-cytoskeletal dynamics within the mammary epithelium. *J. Cell Biol.* 208, 351–366.
- Rodgers, J.T., King, K.Y., Brett, J.O., Cromie, M.J., Charville, G.W., Maguire, K.K., Brunson, C., Mastey, N., Liu, L., Tsai, C.-R., et al. (2014). mTORC1 controls the adaptive transition of quiescent stem cells from G0 to GAlert. *Nature* 510, 393–396.
- Ross, S.R., Hsu, C.L., Choi, Y., Mok, E., and Dudley, J.P. (1990). Negative regulation in correct tissue-specific expression of mouse mammary tumor virus in transgenic mice. *Mol. Cell. Biol.* 10, 5822–5829.
- Russo, J., Wilgus, G., and Russo, I.H. (1979). Susceptibility of the Mammary Gland to Carcinogenesis. 16.
- Saji, S., Jensen, E.V., Nilsson, S., Rylander, T., Warner, M., and Gustafsson, J.-Å. (2000). Estrogen receptors α and β in the rodent mammary gland. *Proc. Natl. Acad. Sci. U. S. A.* 97, 337–342.

- Schafer, K.A. (1998). The cell cycle: a review. *Vet. Pathol.* *35*, 461–478.
- Schiestl, R.H., and Prakash, S. (1988). RAD1, an excision repair gene of *Saccharomyces cerevisiae*, is also involved in recombination. *Mol. Cell. Biol.* *8*, 3619–3626.
- Schottstedt, V., Blümel, J., Burger, R., Drost, C., Gröner, A., Gürtler, L., Heiden, M., Hildebrandt, M., Jansen, B., Montag-Lessing, T., et al. (2010). Human Cytomegalovirus (HCMV) – Revised*. *Transfus. Med. Hemotherapy* *37*, 365–375.
- Shehata, M., Teschendorff, A., Sharp, G., Novcic, N., Russell, I.A., Avril, S., Prater, M., Eirew, P., Caldas, C., Watson, C.J., et al. (2012). Phenotypic and functional characterisation of the luminal cell hierarchy of the mammary gland. *Breast Cancer Res. BCR* *14*, R134.
- Shore, A.N., Chang, C.-H., Kwon, O.-J., Weston, M.C., Zhang, M., Xin, L., and Rosen, J.M. (2016). PTEN is required to maintain luminal epithelial homeostasis and integrity in the adult mammary gland. *Dev. Biol.* *409*, 202–217.
- Sorkhy, M.A., Craig, R., Market, B., Ard, R., and Porter, L.A. (2009). The Cyclin-dependent Kinase Activator, Spy1A, Is Targeted for Degradation by the Ubiquitin Ligase NEDD4. *J. Biol. Chem.* *284*, 2617–2627.
- Sternlicht, M.D., and Sunnarborg, S.W. (2008). The ADAM17–amphiregulin–EGFR Axis in Mammary Development and Cancer. *J. Mammary Gland Biol. Neoplasia* *13*, 181–194.
- Stewart, T.A., Pattengale, P.K., and Leder, P. (1984). Spontaneous mammary adenocarcinomas in transgenic mice that carry and express MTV/myc fusion genes. *Cell* *38*, 627–637.
- Sun, Y., Chen, X., and Xiao, D. (2007). Tetracycline-inducible expression systems: new strategies and practices in the transgenic mouse modeling. *Acta Biochim. Biophys. Sin.* *39*, 235–246.
- Taneja, P., Frazier, D.P., Kendig, R.D., Maglic, D., Sugiyama, T., Kai, F., Taneja, N.K., and Inoue, K. (2009). MMTV mouse models and the diagnostic values of MMTV-like sequences in human breast cancer. *Expert Rev. Mol. Diagn.* *9*, 423–440.
- Teyssier, F., Bay, J.O., Dionet, C., and Verrelle, P. (1999). [Cell cycle regulation after exposure to ionizing radiation]. *Bull. Cancer (Paris)* *86*, 345–357.
- Thul, P.J., Åkesson, L., Wiking, M., Mahdessian, D., Geladaki, A., Blal, H.A., Alm, T., Asplund, A., Björk, L., Breckels, L.M., et al. (2017). A subcellular map of the human proteome. *Science* *356*, eaal3321.
- Tomkinson, A.E., Bardwell, A.J., Bardwell, L., Tappe, N.J., and Friedberg, E.C. (1993). Yeast DNA repair and recombination proteins Rad1 and Rad10 constitute a single-stranded-DNA endonuclease. *Nature* *362*, 860–862.
- Uhlén, M., Fagerberg, L., Hallström, B.M., Lindskog, C., Oksvold, P., Mardinoglu, A., Sivertsson, Å., Kampf, C., Sjöstedt, E., Asplund, A., et al. (2015). Tissue-based map of the human proteome. *Science* *347*, 1260419.

- Uhlen, M., Zhang, C., Lee, S., Sjöstedt, E., Fagerberg, L., Bidkhori, G., Benfeitas, R., Arif, M., Liu, Z., Edfors, F., et al. (2017). A pathology atlas of the human cancer transcriptome. *Science* *357*, eaan2507.
- Veltmaat, J.M., Ramsdell, A.F., and Sterneck, E. (2013). Positional Variations in Mammary Gland Development and Cancer. *J. Mammary Gland Biol. Neoplasia* *18*, 179–188.
- Visvader, J.E., and Lindeman, G.J. (2006). Mammary stem cells and mammopoiesis. *Cancer Res.* *66*, 9798–9801.
- Visvader, J.E., and Stingl, J. (2014). Mammary stem cells and the differentiation hierarchy: current status and perspectives. *Genes Dev.* *28*, 1143–1158.
- Vonderhaar, B.K., and Greco, A.E. (1979). Lobulo-Alveolar Development of Mouse Mammary Glands Is Regulated by Thyroid Hormones. *Endocrinology* *104*, 409–418.
- Wakefield, L.M., Piek, E., and Böttinger, E.P. (2001). TGF-beta signaling in mammary gland development and tumorigenesis. *J. Mammary Gland Biol. Neoplasia* *6*, 67–82.
- Watson, C.J. (2006a). Key stages in mammary gland development - Involution: apoptosis and tissue remodelling that convert the mammary gland from milk factory to a quiescent organ. *Breast Cancer Res.* *8*.
- Watson, C.J. (2006b). Involution: apoptosis and tissue remodelling that convert the mammary gland from milk factory to a quiescent organ. *Breast Cancer Res. BCR* *8*, 203.
- Watson, C.J., and Burdon, T.G. (1996). Prolactin signal transduction mechanisms in the mammary gland: the role of the Jak/Stat pathway. *Rev. Reprod.* *1*, 1–5.
- Watson, C.J., and Khaled, W.T. (2008). Mammary development in the embryo and adult: a journey of morphogenesis and commitment. *Development* *135*, 995–1003.
- Weber, R.J., Desai, T.A., and Gartner, Z.J. (2017). Non-autonomous cell proliferation in the mammary gland and cancer. *Curr. Opin. Cell Biol.* *45*, 55–61.
- Welm, B.E., Dijkgraaf, G.J.P., Bledau, A.S., Welm, A.L., and Werb, Z. (2008). Lentiviral transduction of mammary stem cells for analysis of gene function during development and cancer. *Cell Stem Cell* *2*, 90–102.
- Willmarth, N.E., and Ethier, S.P. (2008). Amphiregulin as a novel target for breast cancer therapy. *J. Mammary Gland Biol. Neoplasia* *13*, 171–179.
- Yu, Q.C., Verheyen, E.M., and Zeng, Y.A. (2016). Mammary Development and Breast Cancer: A Wnt Perspective. *Cancers* *8*.
- Zhang, L., Adileh, M., Martin, M.L., Klingler, S., White, J., Ma, X., Howe, L.R., Brown, A.M.C., and Kolesnick, R. (2017). Establishing estrogen-responsive mouse mammary organoids from single Lgr5+ cells. *Cell. Signal.* *29*, 41–51.

APPENDICES

Appendix 1 Protocols

Primary Cell Isolation Protocol

DAY 1:

[A.] Prepare Reagents

1. Wash Buffer: 5% FBS/F12

25 ml FBS

5 ml AA

475 ml DMEMF12 or HamF12

500 ml

Filter sterilize.

2. 0.25% Trypsin-EDTA (Invitrogen)

3. Growth media:

250 μ l 1mg/ml insulin (5 μ g/ml final)

50 μ l 1mg/ml hydrocortisone (1 μ g/ml final)

25 μ l 10 μ g/ml EGF (5ng/ml final)

250 μ l 10mg/ml gentamycin (50 μ g/ml final)

500 μ l antifungal/antibiotic

2.5 ml FBS

47 ml HamF12

50 ml

Filter sterilize.

4. Digestion Media

250 μ l AA

25 mg collagenase (1mg/ml)

24.75 ml HamF12

25 ml

Filter sterilize and prepare fresh for each use.

[B.] Isolate MECs from mice

1. For the glands of 3 mice, add ~20ml of wash buffer to a 50ml conical tube.

2. Weigh tube with wash buffer and record. Place on ice.

3. Proceed with dissection, removing the #3, 4, 5 glands, removing the lymph node. Transfer glands to wash buffer on ice.

4. Weigh tubes with tissue, and subtract values to determine grams of tissue.

5. Chop tissue till very pasty---no clumps.

Heather LaMarca 6/07

6. Add the appropriate amount of digestion buffer to each tube: 10 ml/gram of tissue

7. Incubate tissue at 37°C on rocker, at ~50 rpm for about 14 hours. (Place tubes at a 45° angle.)

DAY 2:

8. After digestion is complete, shake digested cells vigorously to loosen cells from fat.

Transfer cells to a 15ml conical tube.

9. Spin at 1000 rpm at for 10' using a swing bucket rotor at RT.

Carefully aspirate supernatant.

10. Resuspend cells in 2ml of 0.25% trypsin-EDTA by pipetting up and down.

Incubate at RT for 5', gently inverting throughout the incubation.

Note: A large fibrous mass will ppt when trypsin is added. Also, the volume of trypsin will vary depending on the size of the pellet. After a few minutes, the media should appear clear rather than thick

and clumpy.

11. Neutralize trypsin with 5ml of wash buffer.

Pass cells through a 70µm filter into a 50ml conical tube. (filtration will get rid of the ppt)

12. Transfer cells back to a 15ml conical tube and bring the volume to 15ml with wash buffer.

Spin at 1000 rpm for 10'.

Carefully aspirate supernatant.

13. Continue washing to ensure that enzymatic activity is stopped (~3-4 times total).

Each time, spin at 300 × g for 5' at RT.

14. Resuspend pellet in 3ml of growth media. Dilute cells 1:10-1:50 and count on a hemacytometer.

Yield: ~2.5 × 10⁶ cells per 0.5 g tissue

Permission

Dear Sir/Madam,

Please accept this letter as my authorization for Mr. Julian Eric Derecichej to use the data co-authored in his Master's thesis within his Results. Please do not hesitate to contact me for further clarification.

Bre-Anne Fifield, PhD
University of Windsor

VITA AUCTORIS

NAME:	Derecichei Eric Iulian
PLACE OF BIRTH:	Oradea, Romania
YEAR OF BIRTH:	1994
EDUCATION:	St. Josephs High School, Windsor, ON, 2012 University of Windsor, B.Sc., Windsor, ON, 2016